PERFORMANCE ANALYSIS OF A ROTARY REGENERATOR

A THESIS

Presented to

The Faculty of the Graduate Division

by

Humberto Eduardo Barrientos-Mendoza

In Partial Fulfillment

of the Requirements for the Degree

Master of Science

in Mechanical Engineering

Georgia Institute of Technology

March, 1971

PERFORMANCE ANALYSIS OF A ROTARY REGENERATOR

Approved:

Chairman

Date approved by Chairman: March 4, 1971

ACKNOWLEDGMENTS

The author wishes to acknowledge his debt to the following people who have helped him in the pursuit and culmination of his graduate work at Georgia Tech.

First, to his father, whose assistance in the author's native country of Venezuela has been his most precious link with his country.

To his wife for being a truthful and friendly companion all through his studies in the United States.

To Dr. P. Desai, his thesis advisor, for proposing the original thesis problem and continued assistance and guidance in preparing the thesis.

To Dr. A. Bergles, for continued encouragement within and without the classroom and for consenting to be on the thesis reading committee.

To Dr. K. V. Prasanna, for several useful comments made to improve the thesis.

To Dr. H. Ward, for agreeing to be on the thesis reading committee and for some valuable suggestions to improve the thesis write-up.

TABLE OF CONTENTS

TABLE OF CONTENTS (Concluded)

LIST OF TABLES

LIST OF ILLUSTRATIONS

NOMENCLATURE

A	surface area, ft^2
C_p	specific heat, Btu/lbm °R
f	coefficient of heat transfer by convection, Btu/hr ft^2 °F
h	specific enthalpy of air, Btu/lbm
k	thermal conductivity of the matrix, Btu/hr ft °F
L	length of the matrix, ft
$\dot{m}$	mass rate flow, lbm/hr
N	number of elements of matrix
NTU	number of heat transfer units
NTUo	modified number of heat transfer units = $\frac{1}{C_{min}}\left[\frac{1}{(1/hA)_c + (1/hA)_h}\right]$
P	pressure, lbf/ft^2
p	free flow area ratio of the matrix = $\frac{\text{free flow cross-sectional area}}{\text{total cross-sectional area}}$
$\dot{Q}$	heat transfer rate, Btu/hr
RHE	rotary heat exchanger
r	radial coordinate in the cylindrical frame of reference
T	temperature, °F
v	specific volume, ft^3/lbm
V	velocity, ft/hr
W	specific humidity, lbm of water/lbm dry air

NOMENCLATURE (Concluded)

z	axial coordinate in the cylindrical frame of reference
x	hot or cold

GREEK LETTERS

$\dot{\phi}$	angular velocity, rad/hr
α	surface area density, ratio of total surface area of the matrix to the volume of the matrix, 1/ft
ϕ	circumferential coordinate in the cylindrical frame of reference
ρ	density, lbm/ft^3

SUBSCRIPTS

a	air
avg	average
c	cold
d	conduction
e	external
h	hot
i	internal
r	rotor or matrix
rw	effective average over rotor and condensed heater
s	at the surface of the matrix
t	total
v	convection
w	water
∞	free stream condition

SUMMARY

This thesis concerns the application of a numerical technique to study the performance characteristics of a periodic-flow heat exchanger, with at least one fluid having sufficiently high relative humidity to cause condensation.

Suitable analytical and numerical models are presented to describe the heat exchange between the fluids and the exchanger. Distribution of temperatures within the matrix of the heat exchanger and thermodynamic properties of the fluids (air) flowing through the exchanger are discussed.

CHAPTER I

INTRODUCTION

Rotary Regenerator Heat Exchanger

A commonly accepted classification of heat exchangers is made on the basis of whether they employ heat storage or not. Commonly termed a regenerator, the former operates by means of a storing material which runs through two heat exchanging media, absorbing heat from the hotter medium and transferring heat to the cooler one, through which it flows. On the other hand, a recuperator is a heat exchanger which does not employ heat storage. It operates by direct heat transmission through a separating wall between two fluids exchanging heat or by two direct heat transfer units, coupled with a transfer fluid circulating in cycles between the hot exchanger unit where the thermal energy is received and the cold exchanger unit where the thermal energy is delivered. Such an exchanger necessitates a simultaneous flow of both the fluids engaged in the mutual heat transfer process.

During the past three or four decades several designs incorporating a rotary matrix for the flow of material through which, in turn, flow two streams of fluids at different temperatures, have been considered. In the past, a primary motivation for heat exchangers of such a design, suitably termed as rotary regenerators, has been their use in gas turbine power systems.

A further classification of rotary regenerators or rotary heat exchangers (RHE) can be made on the basis of whether the flow is axial or radial. Figure 1 depicts schematic representations of the two types of RHE.

A common feature of both of these RHE involves the rotation of a porous matrix from a cold fluid stream into a hot fluid stream in a regular periodic fashion. During the part of the cycle that the metal matrix interacts with the cold stream, the matrix loses part of its internal energy due to the heat transferred from the metal to the cold fluid stream. On a subsequent part of the cycle, when due to its rotation the matrix interacts with the hot fluid stream, the metal regains the internal energy via the heat transferred from the fluid to the matrix. For a given speed of rotation of the matrix, together with the proper mass fluxes of cold and hot streams, it is possible to achieve a steady state periodicity of temperature distribution within the matrix. In other words, at the end of a given cycle, the whole matrix attains the same state as it possessed at the end of the previous cycle. The net effect of such a cycle of operation is the exchange of heat between the hot and the cold fluid streams. In principle, this facilitates the cooling of a warm stream or the heating of a cold one, whichever serves the purpose in a particular application.

A perspective view of a typical matrix arrangement in the axial flow type of RHE is shown in Figure 2. Two advantageous features of such a design concern its compactness and the tendency of self cleaning. The heat transfer area per unit volume or the surface area density in such an

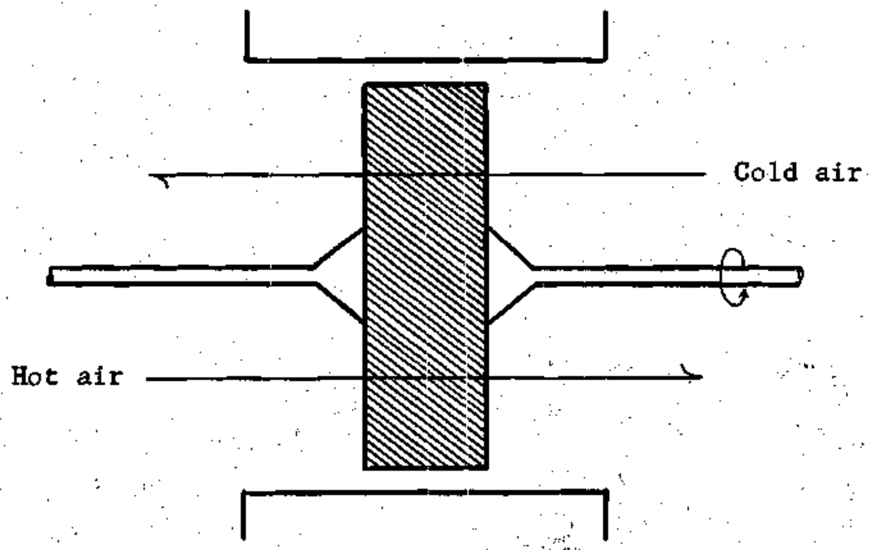

AXIAL FLOW

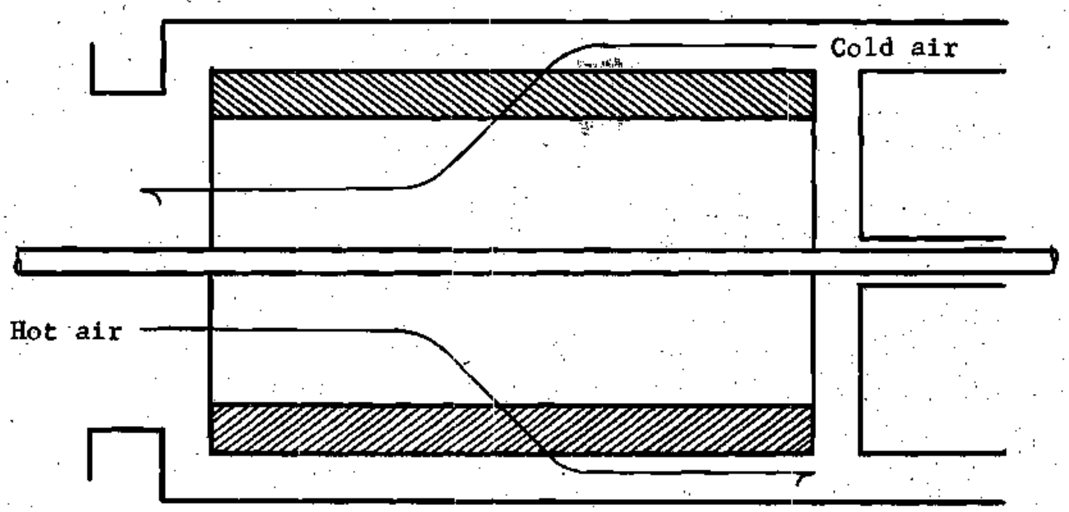

RADIAL FLOW

Figure 1. Rotary Heat Exchanger

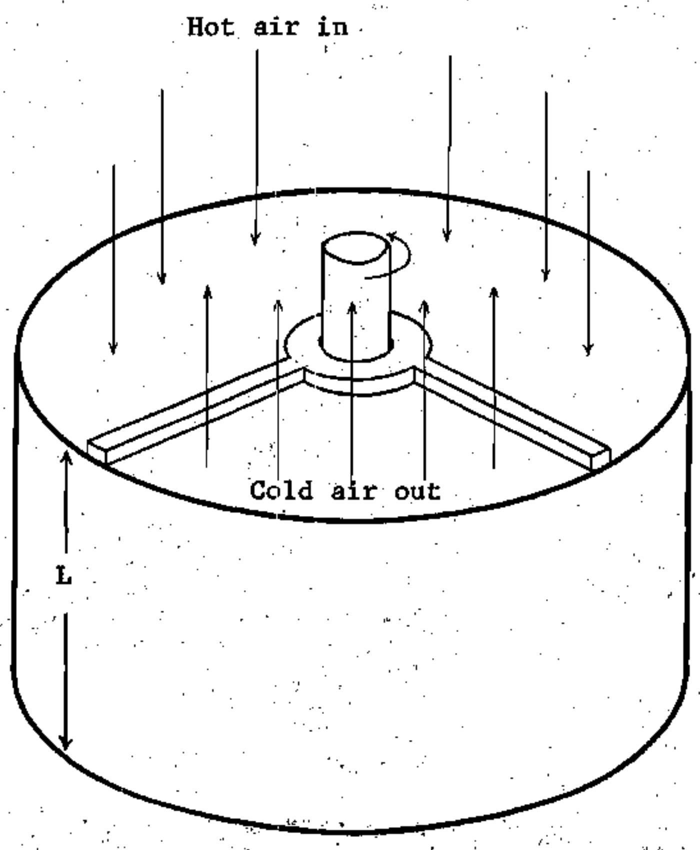

Figure 2. Matrix of a Rotary Heat Exchanger

exchanger is higher than that in a conventional exchanger, thus requiring less volume for a given heat transfer area; this is related to the structure of the porous matrix. Since the axial direction of flow through a particular sector of the matrix is reversed during each cycle, such a geometry provides the self-cleaning feature.

A Brief Survey of Pertinent Literature

Well through the 1930's, two procedures were employed to predict the performance of regenerators (1). One of these procedures was to use empirical data to set up approximate equations by means of which the performance of the regenerator could be predicted. However, because of the nature of the empirical analysis, these equations were only fair approximations for those cases similar to the ones for which the empirical data were obtained. Naturally, they could not be used for other specific cases. The other procedure was based upon analytically or numerically derived solutions of the problem. This last method proved to be very successful and it is being adopted even at present.

Hausen (2) analyzed the problem of RHE by the so-called heat-pole method. He considered the thermal conductivity of the metal of a cylindrical shaped matrix negligible in the direction of air flow (axis of cylinder) and to be infinite in the radial direction. He also considered the heat capacity rate (product of mass flow rate and specific heat) of the hot air flowing through the RHE to be the same as that for the cold matrix itself. He further assumed a unity value for the ratio of the heat conductance of the cold side to the heat conductance of the hot side. By considering the matrix to be divided into an equal number of strips, he obtained the dimensionless temperature distribution, as well as the total heat transfer rate and the regenerator efficiency. He found that the solution converged very quickly with an increase in the number of strips, namely 0.1 percent deviation between calculated efficiencies for nine and for ten strips.

In the 1940's the aircraft industry showed a great interest in the rotary regenerator as a direct application to improving the performance of gas turbines. Substantial attention was focused on the effect of leakage on regenerator effectiveness, and a consequent development of satisfactory seals to minimize leakage, and on the role played by such parameters as the matrix dimensions, as well as the velocities and heat transfer coefficients associated with the problem.

Harper and Rohsenow (3) showed that, in gas turbine applications of the RHE, most of the leakage occurred not by carry-over of the matrix but through the seals of the matrix from the high pressure stream to the low pressure one. In their paper the change of efficiency of the regenerator was evaluated, by considering a relative change of temperature of the discharging stream due to leakage as compared with that for the case of no leakage. This change of efficiency was shown to be rather small, about 1.3 percent corresponding to a 10 percent leakage. They also showed that the effectiveness of the regenerator appeared to increase to a maximum with an increase in thickness of the matrix, beyond which the thermodynamic efficiency of the gas turbine cycle was observed to drop due to an increase in loss of pressure.

The influence of gas stream velocities and mass flow rates on the heat transfer characteristics of the matrix was determined by Tong and London (4) for various matrix structures. Their work was primarily of an empirical nature, with the results expressed as plots of four dimensionless parameters, namely, the drag coefficient, the friction factor, the Reynolds number, and the Prandtl number.

The search for analytical means to predict the performance of the periodic flow regenerator was continued by Coppage and London (5) in a paper where they first made a survey of the different available solutions for the design of regenerators, and then developed a closed form approximate solution of their own which incorporated the work of previous investigators.

Dusinberre (5), in his discussion of the paper by Coppage and London, suggested that, by dividing the matrix of a regenerator into a number of small elements, each element being treated as a cross flow heat exchanger, the efficiency of the regenerator could be calculated for a given set of physically meaningful parameters. Indeed, this was a very useful and powerful suggestion. Lambertson (6) executed Dusinberre's suggestion and developed a finite difference numerical technique, thus contributing significantly toward the solution of the problem, which had eluded many previous investigators. His solutions were useful for a variety of gas turbine applications.

Lambertson's work forms a commonly accepted basis for design data for the periodic flow type of heat exchanger and has been incorporated by Kays and London (7) in their textbook on compact heat exchangers. It is worth noting that the influence of axial conduction had not been included in Lambertson's work. It was generally accepted that axial conduction of heat might be a significant consideration for high performance regenerators.

Bahnke and Howard (8) carried out Dusinberre's suggestion in a fashion similar to that by Lambertson, but they included the effect of longitudinal heat conduction in the heat exchanger. It was shown in their paper that, for a regenerator effectiveness lower than 90 percent, axial conduction did not play a significant role in the overall heat transfer mechanism. However, they showed that, for effectiveness higher than 90 percent, the influence of axial heat conduction was progressively important in the computation of effectiveness and heat transfer units.

Recent years have seen a considerable increase of interest in utilizing the rotary regenerators beyond the classical gas turbine applications. Drying and air conditioning systems are but two of the more prominent cases where the use of rotary regenerators may show considerable promise. In such applications, the hot and cold streams of air, owing to their thermodynamic states, involve condensation of the water vapor flowing with the air. In an attempt to establish the applicability of a rotary regenerator to a clothes drying process, Mercure (9) performed simple thermodynamic computations to evaluate its performance. In such an application, room air sucked through a sector of the regenerator matrix and passed through an electric heater is supplied to the drum of the clothes dryer. After absorbing moisture from a wet load of clothes, the hot, humid air is passed through another sector of the matrix, and is subsequently exhausted into the ambient. The rotary matrix absorbs heat from the hot stream, stores the energy, and returns it to the incoming cold stream in a periodic fashion. In the process, a certain amount of condensate is undesirably carried over from the hot sector to the cold one. Due to its simplistic nature, Mercure's computational procedure did not allow a prediction of regenerator effectiveness based on simultaneous condensation and convective heat transfer. No other references to the analyses of a rotary heat exchanger in the presence of condensing water vapor on the matrix are available in the literature at present.

Statement of the Proposed Problem

The object of this study is to investigate the application of a finite difference numerical technique to the performance analysis of an RHE with humid air flowing through it. The approach adopted for this investigation consists of developing a technique to predict the variable humid air properties leaving the regenerator for a given state of entering air, with the results coupled to an effectiveness analysis capable of predicting the performance of the rotary regenerator.

CHAPTER II

DEVELOPMENT OF THE ANALYTICAL MODEL

Selection of the Coordinate System and the Differential Control Volume

The physical geometry of the domain of interest in this analysis, namely a cylindrical matrix of a rotary heat exchanger, suggests the use of a cylindrical coordinate frame. The origin is taken at the center of the top of the matrix. The positive z direction is measured downward along the axis of symmetry. The variable r is measured outward along the radius of the cylinder, and ϕ is measured positive in the counter-clockwise direction. With reference to such a coordinate frame, the domain of the matrix can be defined as:

$$\begin{aligned} r_i \leqq\ & r \leqq r_e\ , \\ 0 \leqq\ & \phi \leqq 2\pi\ , \\ 0 \leqq\ & z \leqq L\ . \end{aligned} \tag{2-1}$$

A differential control volume fixed in space and referred to the cylindrical coordinate frame is shown in Figure 3.

As the matrix rotates, its elements may be considered to enter and leave the differential control volume in a periodic fashion. The control volume is considered to be interacting with its surroundings in the following fashion:

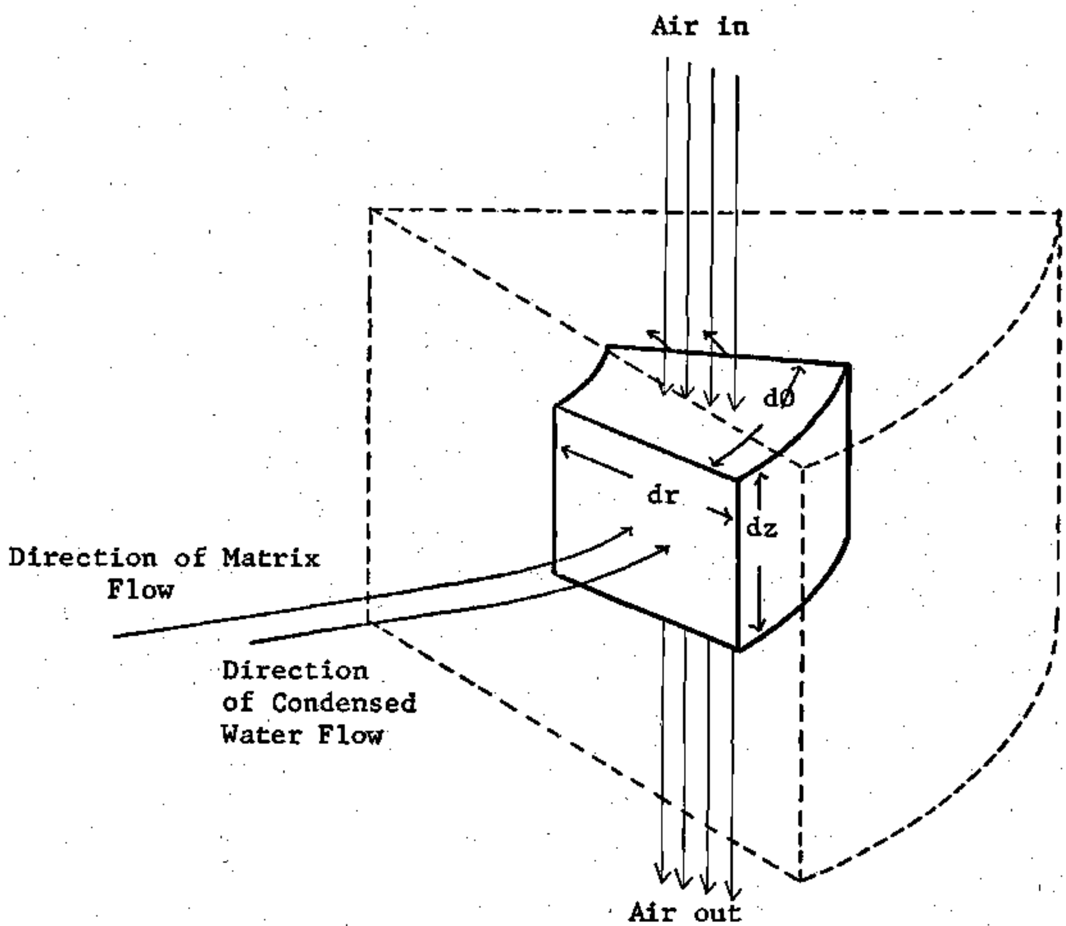

Figure 3. Differential Volume Element of the Matrix

Matrix and water enter and leave the control volume along the ϕ direction at constant velocity, thus resulting in transport of heat and mass across the control surface. Humid, hot air enters through the top and leaves through the bottom of the control volume along the positive z direction at constant flow rate, with mass and energy transport taking place, as explained above. Heat transfer by conduction enters the three positive faces and leaves through the three opposite faces of the control surface.

Governing Equations and Boundary Conditions

A steady state heat balance over the control volume may be expressed, in words, as

(Net conduction heat transfer into the C.V.) + (Net heat transfer in, due to the matrix and water mass entering and leaving the C.V.) + (Net heat transfer due to the air entering the top and leaving through the bottom of the C.V.) = 0. (2-2)

This same equation, written on a per unit volume basis in terms of symbols, gives

$$\left[k_r \left(\frac{\partial^2 T}{\partial r^2} + \frac{1}{r}\frac{\partial T}{\partial r}\right) + \frac{k_\phi}{r^2}\frac{\partial^2 T}{\partial \phi^2} + k_z \frac{\partial^2 T}{\partial z^2}\right](1 - p) - \tag{2-3}$$

$$\frac{\partial}{\partial \phi}(p\ \rho_{rw}\ C_{prw}\ \dot{\phi} T) + p\ \rho_a V_a \frac{\partial h_\infty}{\partial z} = 0 .$$

Following Stoecker (10), the differential heat transfer from the humid air to the C.V. is

$$d\dot{Q}_a = \frac{f}{C_{pm}} (h_\infty - h_s)\ dA\ , \qquad (2\text{-}4)$$

and

$$d\dot{Q}_a = p\ \rho_a V_a \frac{\partial h_\infty}{\partial z} r d\phi dr dz\ . \qquad (2\text{-}5)$$

The differential surface area available for convective heat transfer is

$$dA = \alpha r \phi dr dz\ , \qquad (2\text{-}6)$$

where α is the surface area density, or the ratio of total surface area of the matrix to the volume of the matrix.

When equations (2-4), (2-5), and (2-6) are combined, one obtains

$$\frac{f}{C_{pm}} (h_\infty - h_s)\ dA = p\ \rho_a V_a \frac{\partial h_\infty}{\partial z} \frac{dA}{\alpha}\ . \qquad (2\text{-}7)$$

The boundary condition for enthalpy may be specified as

$$\left.\begin{array}{l} 0 \leqq \phi \leqq \phi_h \\ z = 0 \end{array}\right\} \quad h(r,\phi) = \text{constant}\ . \qquad (2\text{-}8)$$

The interval of existence of ϕ in equation (2-8) specifies the hot sector side of the matrix.

In a similar fashion, for the cold side of the matrix, the boundary condition may be written as

$$\left.\begin{array}{l} \phi_h \leq \phi \leq 2\pi \\ z = L \end{array}\right\} \quad h(r,\phi,L) = \text{constant.} \tag{2-9}$$

In these equations,

$$T = T(r,\phi,z),\ h_\infty = h_\infty(T,P_a),\ \text{and}\ \rho_a = \rho_a(T,P_a)\ . \tag{2-10}$$

It may be pointed out that the summation of partial pressures of air and water yields the constant value of the total pressure, P_t.

Equations (2-3) together with the differential energy balances stated in equations (2-4) and (2-5) as well as the boundary conditions expressed by equations (2-8) and (2-9) represent an analytical model of the problem.

Simplification of the Analytical Model

A closed form analytical solution of the preceding system of equations proves to be a formidable task. It is recognized that enthalpy and density are not known *a priori* as a function of spatial location; moreover, if spatial location is not involved, these properties are nonlinear functions of temperature and pressure.

These equations are elliptic-type partial differential equations. Classical mathematical techniques have been often employed with special treatment of this type of equation. However, general solutions for elliptic-type partial differential equations are not available.

It is fortunate that some reasonable idealizations that do not significantly affect the engineering applicability of the equations can be made to simplify the problem. Following such simplifications, it is feasible to develop a finite difference model of the equations, which can be solved by using numerical solution techniques.

Consider the following idealizations with subsequent justifications of the same:

1) The two fluid streams through the matrix represent a counter-flow energy exchange system.

2) The thermodynamic properties of the entering fluids are uniform over the flow inlet cross sections and these properties remain constant with time.

3) The convection heat transfer coefficients are constant along a flow line.

4) The thermal properties of the matrix are invariant with changes of temperature and time.

5) No mixing of the hot and cold fluid streams occurs, either as a result of direct leakage or due to carry over.

6) Regular periodicity exists for all properties within the matrix elements, yielding quasi-steady conditions.

7) The matrix rotates at a constant angular velocity.

8) The water condensed at a particular station within the matrix remains there until reevaporated and the temperature of the condensed water is assumed to be equal to the temperature of the matrix in which the water rests.

9) The thermal conductivity of the porous matrix is negligibly small in the circumferential direction and extremely large in the radial direction. Thus, heat by conduction in the circumferential direction may be neglected, and the temperature along a radius may be assumed constant.

Since the first three assumptions are very commonly used and justified in the literature on the subject, it is not necessary to elaborate on those any further.

The fourth assumption implies that the density, specific heat, and other thermal properties of the metal matrix are independent of temperature. This is reasonable to accept for the range of temperatures in such applications as drying and air conditioning processes considered in this investigation.

The fifth assumption is well approximated when the width of the matrix is small, as is usually encountered in RHE to minimize pressure losses; or if the air velocity is high compared with the velocity of rotation of the matrix, the approximation represents the physical picture reasonably well. For example, with an air velocity of 700 ft/min through a one inch thick matrix turning at 15 rpm, the dead angle is around 0.64 degrees, which approximately equals 0.4 percent of one turn of rotation. Moreover, it must be recognized that, in a drying process, both flow streams have about the same total pressure, rendering a low driving potential for leakage flow. This, of course, is not the case in gas turbine applications, where the pressure ratio is quite high.

The sixth assumption corresponds to the quasi-steady state of the system. The transient state at the start of operation tends to reach a quasi-steady state as the number of cycles of operation increases. In other words, after a certain number of cycles, the system, from an engineering point of view, becomes one in steady state, provided that there is no storage of water condensed from the hot fluid stream on the matrix. For the case with condensation, the following sequence of operation results in a reevaporation of the condensate: Water collected on the matrix is carried along by the matrix to a region where the temperature is higher. The specific humidity of air in contact with the condensate in this region is higher than the specific humidity of free stream air in the region. As a result, a mechanism similar to the evaporation of water from the wick around a wet bulb occurs causing the evaporation. If the condensed water does not reevaporate during one complete turn, there will be successive accumulations of condensed water during each turn, still allowing an eventual steady state system with water in the liquid phase being carried over beyond the matrix by the air stream. Such an amount of condensation need not be anticipated for the case under study.

The ninth idealization is based on the relatively small order of magnitude of circumferential temperature gradient compared with that in the axial direction. The thermal conductivity is assumed to be very large in the radial direction, since with all the other idealizations, the matrix elements along a particular radius have the same governing equations, the same boundary conditions, and the same time of exposure to both hot and cold streams. This results in a constant temperature along a radius. The matrix thus behaves as if the thermal conductivity along a radius were infinite.

A Note on the Qualitative Temperature Distribution Within the Matrix

During the hot cycle a sector of the matrix raises its temperature at a faster rate initially and at a slower rate toward the end, the latter caused by a diminishing temperature differential between the matrix and the hot stream of fluid. In a similar fashion during the cold cycle the matrix lowers its temperature at a faster rate initially and at a slower rate toward the end.

The temperature distribution within the matrix at the beginning of the hot cycle is the same as that at the end of the cold cycle, since the spatial positions of the matrix for the two cases are identical. This is usually referred to as the reversal condition. Finally, the mean temperature of the matrix lies somewhere between the mean entering temperatures of the hot and cold streams.

Simplified Analytical Model

With the idealizations that have been made, the following simplifications are possible.

Idealization nine, namely that the thermal conductivity of the matrix in the circumferential direction is negligibly small, implies that the heat transfer by conduction is negligible and that

$$\frac{k_\phi}{r^2}\frac{\partial^2 T}{\partial \phi^2} = 0 \; . \qquad (2\text{-}11)$$

Similarly, if the temperature along a radius may be assumed to be constant, one obtains

$$\frac{\partial T}{\partial r} = \frac{\partial^2 T}{\partial r^2} = k_r \left(\frac{\partial^2 T}{\partial r^2} + \frac{1}{r}\frac{\partial T}{\partial r}\right) = 0 \ . \qquad (2\text{-}12)$$

From idealization number seven one obtains a constant angular velocity of the matrix, i.e., $\dot{\phi}$ = constant.

When these assumptions are incorporated into equation (2-3), the resulting equation becomes

$$k_z(1 - p)\frac{\partial^2 T}{\partial z^2} - \frac{\partial}{\partial \phi}(p\ \rho_{rw}\ C_{prw}\ \dot{\phi}T) + p\ \rho_a V_a \frac{\partial h_\infty}{\partial z} = 0 \ . \qquad (2\text{-}13)$$

The boundary conditions for enthalpy expressed by equations (2-8) and (2-9) remain unchanged. Thus, the analytical formulation of the transport of mass and heat in a rotary regenerator with condensing vapor is represented by equations (2-7) and (2-13), together with the boundary conditions expressed by equations (2-8) and (2-9).

CHAPTER III

DEVELOPMENT OF THE NUMERICAL MODEL

The Grid System

For the purpose of developing a scheme of difference equations, the matrix is divided into N_r axial planes and $(N_h + N_c)$ radial planes around the circumference of the matrix. A total number of $N_r(N_h + N_c)$ elements, each element resembling the differential control volume discussed in Chapter II, are thus formed. It may be pointed out that, by distinguishing between the hot and cold sides of the matrix and by opening or developing the circular geometry onto a plane, the numerical analysis procedure can be carried out in the classical manner. The overall grid configuration bears a resemblance to a layered cake, as shown in Figure 4. The developed view of the grid system is shown in Figure 5.

The temperatures on the left and on the right sides of each element of the matrix are defined by a row-column system, the generic subscripts being i for rows and j for columns. The same generic system of description is used for the properties and states of the humid air at the top and bottom of each element. In other words, the generic subscript i implies a row and the generic subscript j implies a column. This scheme avoids any confusion and is simple because any reference to temperatures implies the left-right sides of the element, whereas all air states and properties refer to the top-bottom sides of the element.

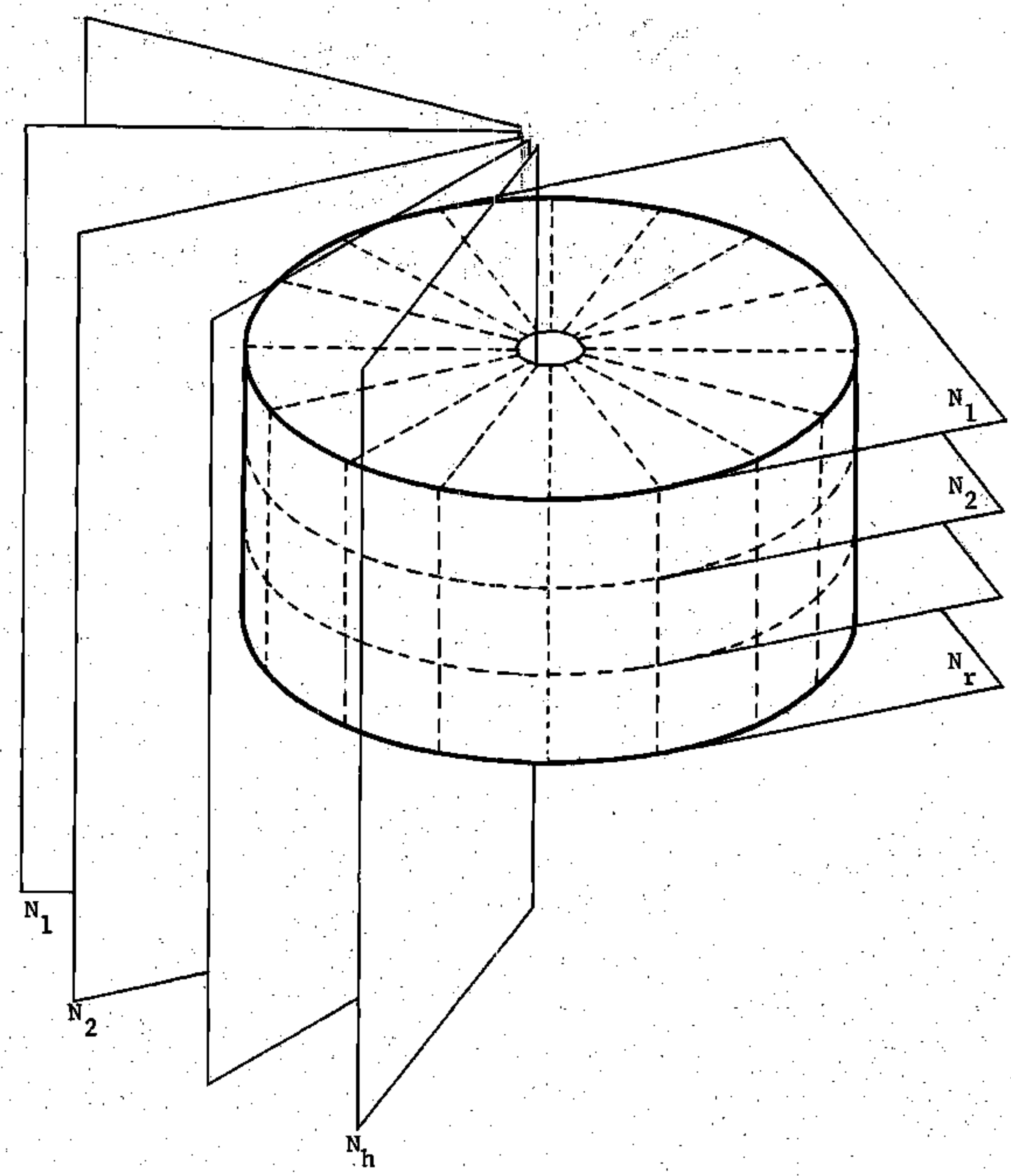

Figure 4. Matrix Divided into Elements

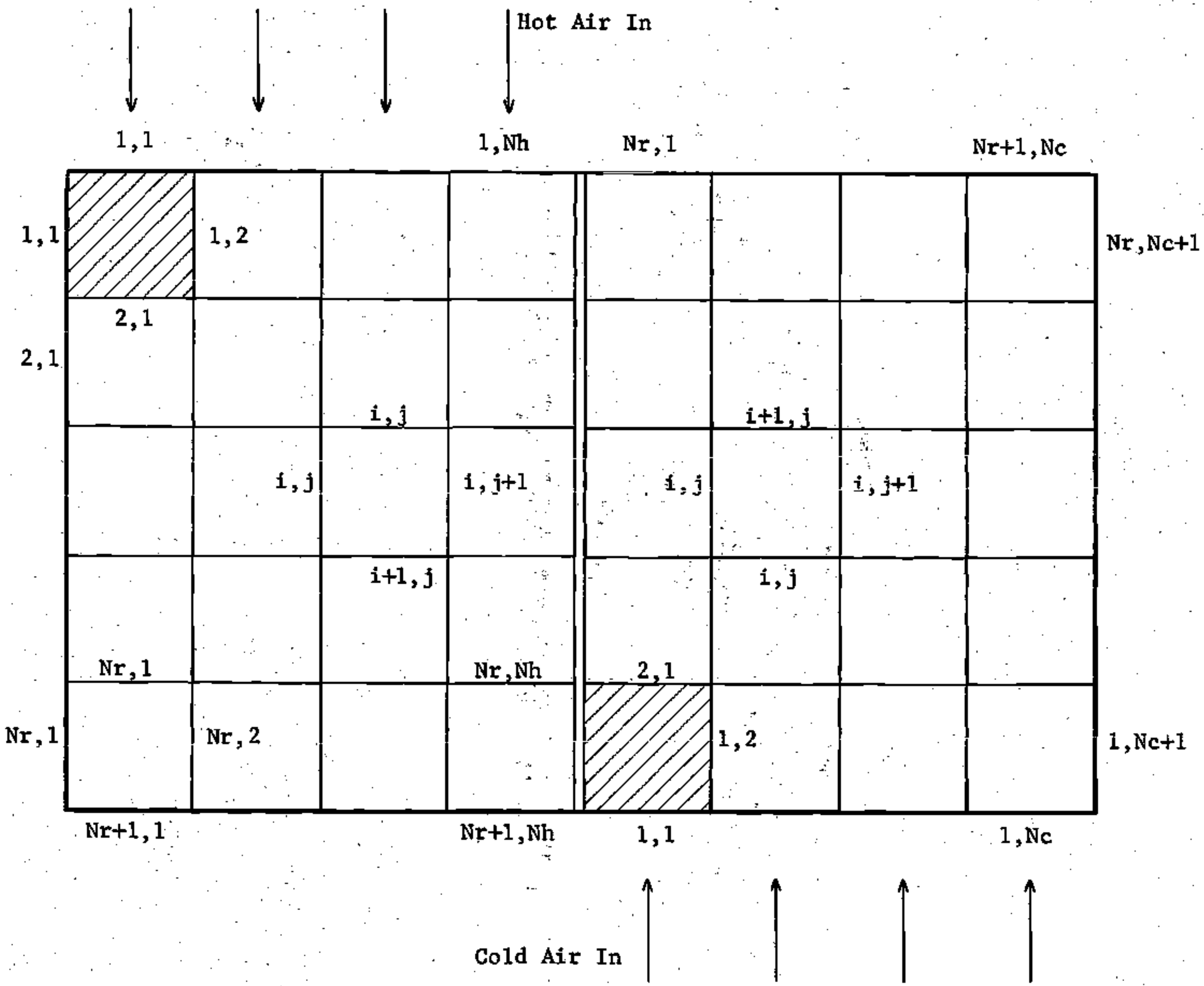

Figure 5. Developed Matrix

Finite Difference Approximation of the Analytical Model

It was pointed out in Chapter II that even the simplified analytical model leads to a system of differential equations for which a closed form solution is not available. A finite difference approximation of the model is therefore deemed necessary.

To proceed along these lines, equation (2-13) is first multiplied by the differential volume $rd\phi drdz$ to yield

$$k_z(1 - p) \frac{\partial^2 T}{\partial z^2} rd\phi drdz - \frac{\partial}{\partial \phi} (p\ \rho_{rw}\ C_{prw}\ \dot{\phi} T)\ rd\phi drdz - \tag{3-1}$$

$$p\ \rho_a V_a \frac{\partial h_\infty}{\partial z} rd\phi drdz = 0\ .$$

It was pointed out that $(1 - p)\ rd\phi dr$ is the area of the differential element available for conduction, which is denoted by dA_d. The factor $(1 - p)$ is included to account for the porosity of the material of the matrix. $pdrdz$ is the area through which water and matrix enter the differential volume. $prd\phi dr$ is the area through which air enters the differential volume.

The mass flow rate for air is given by

$$\dot{m}_a = \rho_a V_a\ A = \rho_a V_a\ prd\phi dr\ , \tag{3-2}$$

and the mass flow rate of the matrix element is given by

$$\dot{m}_r = \rho_r V_r\ A = \rho_r V_r\ pdrdz\ ,$$

where $$V_r = r\dot{\phi} \; . \tag{3-4}$$

A combination of equations (3-3) and (3-4) gives

$$\dot{m}_r = \rho_r \, r\dot{\phi} \; pdrdz \; . \tag{3-5}$$

The first term of equation (3-1), $k_z \frac{\partial^2 T}{\partial z^2} [(1-p) \; rd\phi dr] \; dz$, may be replaced by its equivalent $k_z \frac{\partial^2 T}{\partial z^2} dA_d \; dz$, or

$$k_z \frac{\partial^2 T}{\partial z^2} [(1-p) \; rd\phi dr] \equiv k_z \frac{\partial^2 T}{\partial z^2} dA_d \; dz \; . \tag{3-6}$$

Contributions from water flow rate and matrix flow rate to the second term of equation (3-1) may be isolated to result in

$$\frac{\partial}{\partial \phi} [\rho_{rw} \; C_{prw} \; \dot{\phi} T] \; prd\phi drdz \equiv \dot{m}_r \; C_{pr} \frac{\partial T}{\partial \phi} d\phi + C_{pw} \frac{\partial (\dot{m}_w T)}{\partial \phi} d\phi \; . \tag{3-7}$$

It may be noted that the mass flow rate of water depends on an increase or decrease in the rate of condensation or evaporation. On the other hand, the mass flow rate of rotor is a constant quantity.

The third term of equation (3-1) may be expressed with the use of equation (3-2) as

$$p \rho_a V_a \frac{\partial h_\infty}{\partial z} rd\phi drdz \equiv \dot{m}_a \frac{\partial h_\infty}{\partial z} dz \; . \tag{3-8}$$

Incorporation of identities (3-6), (3-7), and (3-8) into equation (3-1) gives

$$k_z \frac{\partial^2 T}{\partial z^2} dA_d\ dz - \dot{m}_r\ C_{pr} \frac{\partial T}{\partial \phi} d\phi - C_{pw} \frac{\partial(\dot{m}_w T)}{\partial \phi} d\phi - \tag{3-9}$$

$$\dot{m}_a \frac{\partial h_\infty}{\partial z} dz = 0 .$$

In a similar fashion equation (2-10) may be expressed in the form

$$\dot{m}_a \frac{\partial h_\infty}{\partial z} dz = \frac{f}{C_{pm}} (h_\infty - h_s)\ dAv , \tag{3-10}$$

where the surface area density is again taken into account to obtain the available area for convection.

The boundary conditions for enthalpy remain the same as those given by equations (2-8) and (2-9).

To transform equations (3-9) and (3-10) into finite difference forms, the differentials may be substituted by finite increments by referring to the grid system developed earlier.

The amounts of air entering the hot and cold sides of an element of matrix are, respectively, $\dot{m}_{ah}/N_h$ and $\dot{m}_{ac}/N_c$.

The convection area for each element equals the total area for convection of one side of the matrix divided by the total number of elements on that size, viz.,

$$\Delta Av_h = \frac{Av_h}{N_r\ N_h} \quad \text{and} \quad \Delta Av_c = \frac{Av_c}{N_r\ N_c} ; \tag{3-11}$$

$$\Delta A_{dh} = \frac{A_{dh}}{N_c} \quad \text{and} \quad \Delta A_{dc} = \frac{A_{dc}}{N_c} . \tag{3-12}$$

The length of each element is the total length of the matrix divided by the number of rows of the matrix, or

$$z = L/N_r , \tag{3-13}$$

and it is the same for each side of the matrix.

Figure 6 represents an enlarged view of a portion of the overall grid system, and indicates the assigned values of temperatures and enthalpies.

It is recognized that

$$\frac{d^2T}{dz^2} = \frac{d}{dz}\left[\lim_{\Delta z \to 0} \frac{T(z) - T(z - \Delta z)}{\Delta z}\right] = \tag{3-14}$$

$$\lim_{\Delta z \to 0} \frac{1}{\Delta z}\left[\frac{T(z + \Delta z) - T(z)}{\Delta z} - \frac{T(z) - T(z - \Delta z)}{\Delta z}\right].$$

When equation (3-14) is applied to the dashed element of Figure 7 one obtains

$$\frac{d^2T}{dz^2} = \lim_{\Delta z \to 0}\left[\left(\frac{T(i-1,j) + T(i-1,j+1)}{2} - \frac{T(i,j) + T(i,j+1)}{2}\right) - \right. \tag{3-15}$$

$$\left.\left(\frac{T(i,j) + T(i,j+1)}{2} - \frac{T(i+1,j) + T(i+1,j+1)}{2}\right)\right]\frac{1}{\Delta z^2} .$$

By similar logic the circumferential temperature gradient may be expressed by

$$\frac{dT}{d\phi} = \lim_{\Delta\phi \to 0} \frac{T(i,j+1) - T(i,j)}{\Delta\phi} . \tag{3-16}$$

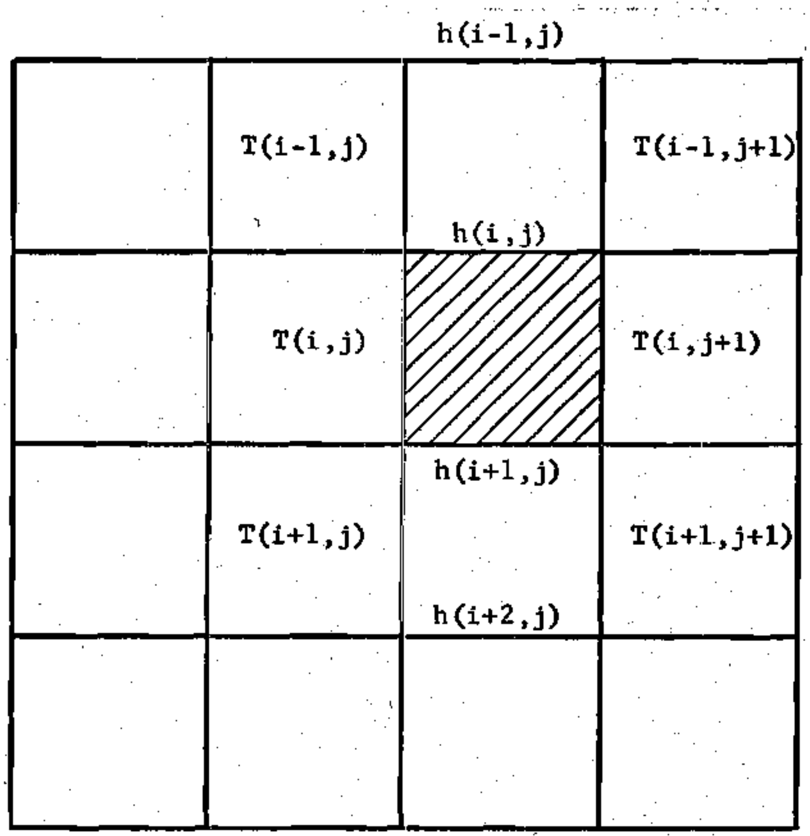

Figure 6. Enlarged View of a Segment of Developed Matrix

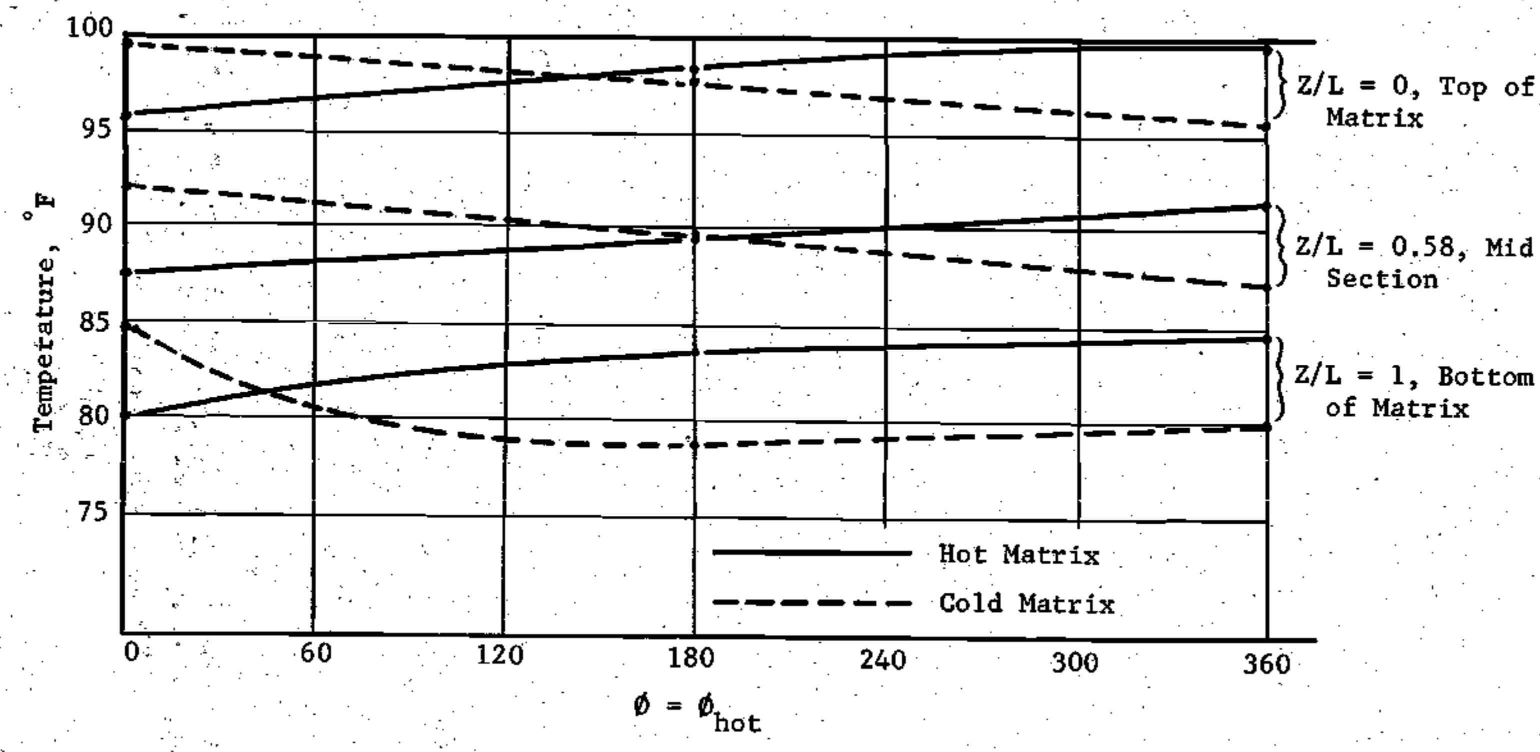

Figure 7. Angular Displacement Along Developed Matrix, ϕ, Degrees

The circumferential gradient of the quantity ($\dot{m}_w T$) may also be expressed, with a few algebraic manipulations, as

$$\frac{d(\dot{m}_w T)}{d\phi} = \lim_{\Delta\phi \to 0} \frac{\dot{m}_w(\phi+\Delta\phi)\ T(\phi+\Delta\phi) - \dot{m}_w(\phi)\ T(\phi)}{\Delta\phi} = \tag{3-17}$$

$$\lim_{\Delta\phi \to 0} \left[\frac{\dot{m}_w(i,j+1)\ T(i,j+1) - \dot{m}_w(i,j)\ T(i,j)}{\Delta\phi}\right].$$

Likewise,

$$\frac{dh_\infty}{dz} = \lim_{\Delta z \to 0} \left(\frac{h_\infty(i+1,j) - h_\infty(i,j)}{\Delta z}\right). \tag{3-18}$$

Incorporation of equations (3-12) through (3-18) into equations (3-9) and (3-10) yields

$$\frac{N_r}{N_x} \frac{k}{2} \frac{A_d}{L} \Big[(T(i-1,j) + T(i-1,j+1) - 2(T(i,j) + T(i,j+1)) + \tag{3-19}$$

$$(T(i+1,j) + T(i+1,j+1)\Big] - \frac{\dot{m}_r C_{pr}}{N_r} \Big[T(i,j+1) - T(i,j)\Big] -$$

$$C_{pw} \Big[\dot{m}_w(i,j+1)\ T(i,j+1) - \dot{m}_w(i,j)\ T(i,j)\Big] - \frac{\dot{m}_a}{N_x} \Big[h_\infty(i+1,j) - h_\infty(i,j)\Big]$$

$$= 0 .$$

A further simplification is

$$N_h = N_c = N_r = N . \tag{3-20}$$

Incorporation of equation (3-20) and a rearrangement yields

$$\frac{\dot{m}_r\, C_{pr}}{N_r}\left[T(i,j+1) - T(i,j)\right] + \left[\dot{m}_w(i,j+1)\, C_{pw}\, T(i,j+1) - \dot{m}_w(i,j)\, C_{pw}\, T(i,j)\right] - \frac{\dot{m}_a}{N_x}\left[h_\infty(i,j) - h_\infty(i+1,j)\right] + \frac{kA_d}{2L} \times \left[(T(i-1,j) + T(i-1,j+1)) - 2(T(i,j) + T(i,j+1)) + (T(i+1,j) + T(i+1,j+1))\right] = 0 \,. \tag{3-21}$$

Similar manipulations of equation (3-10) yield

$$\dot{m}_a\left[h_\infty(i+1,j) - h_\infty(i,j)\right] = \frac{fAv}{C_{pm}\, N_x}\left[\frac{h_\infty(i,j) + h_\infty(i+1,j)}{2} - h_{savg}\right] . \tag{3-22}$$

Equations (3-21) and (3-22) can be readily applied to any specific element in the matrix. If all the entering conditions of an element are assumed, the problem resolves to determining the unknown exit conditions. In order for this system of equations to be compatible and determinate, four more equations are needed. These are:

a) Conservation of mass equations

$$\frac{\dot{m}_a}{N_x}\left[W(i,j) - W(i+1,j)\right] = \dot{m}_w(i,j+1) - \dot{m}_w(i,j) \,, \tag{3-23}$$

and

$$\dot{m}_a \left[W(i,j) - W(i+1,j)\right] = \frac{fAv}{C_{pm}\, N_r}\left[\frac{W(i,j) + W(i+1,j)}{2} - W_{savg}\right] . \qquad (3\text{-}24)$$

b) Psychrometric equations

$$h = h(T,P) \ , \qquad (3\text{-}25)$$

and

$$W = W(T,P) \ . \qquad (3\text{-}26)$$

Equations (3-21) through (3-26) may be applied to the cold side or to the hot side of the matrix by appropriate replacement of subscript x by c or h, respectively.

This set of equations is further simplified (see Appendix I) to yield

$$h_\infty(i+1,j) = h_\infty(i,j) - HC81\ [W(i,j) - W_{savg}(i,j)]\ C_{pw}\ T(i,j) \qquad (3\text{-}27)$$

$$[HC82\ \dot{m}_w(i,j)\ C_{pw} + HC83][T(i,j+1) - T(i,j)] -$$

$$HC84\ [(T(i-1,j) + T(i=1,j+1)) - 2(T(i,j) + T(i,j+1) + (T(i+1,j) +$$

$$T(i+1,j+1))]\ ,$$

and

$$h_\infty(i+1,j) = h_\infty(i,j) + HC81\ [h_{savg}(i,j) - h(i,j)]\ . \qquad (3\text{-}28)$$

In equations (3-27) and (3-28)

$$HC81 = \frac{2B}{N + B}\ , \qquad (3\text{-}29)$$

$$HC82 = \frac{N}{\dot{m}_a}\ , \tag{3-30}$$

$$HC83 = \frac{\dot{m}_r\ C_{pr}}{\dot{m}_a}\ , \tag{3-31}$$

$$B = \frac{fAv}{2\ \dot{m}_a\ C_{pm}}\ , \tag{3-32}$$

and

$$HC84 = \frac{k\ A_d}{2\ \dot{m}_a L}\ . \tag{3-33}$$

A Note on Uniqueness and Stability of the Solution

Equations (3-27) and (3-28) have two unknowns, $h_\infty(i+1,j)$ and $T(i+1,j)$. It may be seen that, in equation (3-27), $h_\infty(i+1,j)$ diminishes when $T(i,j+1)$ increases, and, in equation (3-28), $h_\infty(i+1,j)$ increases when $T(i,j+1)$ increases. This implies that there is only one solution which is unique, provided that the factor $\left(1 - \frac{N - B}{N + B}\right)$ in equation (A-7) in Appendix I is greater than one. A negative value of this factor corresponds to an unrealistic physical conclusion of both the hot air and the matrix losing heat simultaneously. Therefore, a greater value than one of the factor is a valid criterion for a stable solution. In other words, the number of elements into which the matrix is subdivided has to be such that $\left(1 - \frac{N - B}{N + B}\right)$ is greater than one, or $N > B_h$. A similar argument for the cold region leads to the condition $N > B_c$.

CHAPTER IV

PROCEDURAL CONSIDERATIONS FOR NUMERICAL SOLUTIONS

Selection of Numerical Values of Input Parameters

Prior to providing an explanation of the numerical procedure adopted to solve the equations developed in the preceding chapter, it is appropriate to discuss the choice of numerical values assigned to several parameters in this investigation.

The previously stated purpose of this study was to demonstrate the validity of the present numerical technique to analyze the RHE rather than obtain design data for a specific application. It may be pointed out that the adaptability of the present technique is not restricted to a unique set of numerical values assigned to various design parameters.

The states of the entering hot and cold streams depend on the specific applications of the RHE. The numerical values selected for the states of entering hot and cold air (hot air at 100 °F, 60 percent relative humidity; cold air at 80 °F, 50 percent relative humidity), to illustrate the procedure of integration, are within the general range normally found in such applications of the RHE as an air conditioning system and a cloth drying machine. An immediate consequence of the preceding choice of states of entering streams is the specification of their respective enthalpies, specific heats, and specific humidities.

The practical convenience of having approximately the same mass flow rate for dry streams of hot and cold air, together with the ease of comparing trends of the results of this investigation with those reported by Kays and London (7), dictate the choice of the numerical value for the ratio of minimum to maximum heat capacity rates, C_{min}/C_{max}, as 0.7. To ascertain its influence, a value of 0.9 for this parameter was also examined. The mass flow rates for each of the fluid streams consistent with these considerations is approximately 1500 lbm/hr.

Two values for the ratio of the heat capacity rate of the matrix to the minimum heat capacity rate of air, C_r/C_{min}, are considered sufficient to examine the influence of this parameter on the effectiveness of the RHE. These values were selected as two and five, following Kays and London (7).

Use of Psychrometric Equations

Before the numerical technique can be applied to the set of equations derived in Chapter III, it is necessary to have the properties of interest defined by equations of such forms as represented by equations (3-25) and (3-26). Information from steam tables (11) and psychrometric tables (12) can be conveniently used for these formulations. The water vapor properties of interest are the enthalpy and the specific volume as functions of pressure and temperature. Also needed is the saturated water vapor pressure as a function of temperature. The steam tables list all of these properties in a convenient form to adapt into the scheme of computation. It may be noted that the total pressure used in a psychrometric equation is standard atmospheric pressure, or 14.696 lbf/in^2.

It has been assumed that air behaves as an ideal gas yielding the enthalpy

$$h = h(T) \quad . \tag{4-1}$$

Although water vapor deviates from ideal gas behavior, fortunately, the air-water vapor mixture can be still treated as an ideal mixture, with the provision that both air and water vapor occupy the same total volume at the same time. Nevertheless, for the purpose of calculating the dew point temperature, it is reasonable to assume an ideal gas behavior for water vapor. The specific humidity is then given by

$$W = \frac{v_a}{v_w} = C_1 \frac{T}{(P - P_w)\ v_w} = f(T,P_w) \quad . \tag{4-2}$$

In equation (4-2), C_1 is a constant with its numerical value determined by the choice of units, P is the total pressure of the mixture, and P_w is the partial pressure of the water vapor. Equation (4-2) indicates that the specific humidity is a function of temperature and partial pressure of water only.

The enthalpy of the air-water vapor mixture can be expressed as

$$h = h_a + w\ h_w = g(T,P_w) \quad , \tag{4-3}$$

which, again, indicates that the enthalpy of the mixture is a function of temperature and partial pressure of water vapor. The datum temperature for enthalpies can be taken at the standard value of 32°F. Finally, the dew point temperature of the mixture, as a function of temperature and specific humidity, can be determined by knowing the correspondingly partial pressure of water vapor and by employing the relation

$$w = C_2 \frac{P_w}{(P - P_w)} , \tag{4-4}$$

where C_2 is a constant with a value dependent on the particular choice of units. The dew point temperature can be evaluated by identifying the saturation temperature from the steam tables corresponding to the known partial pressure of water vapor.

Numerical Integration Procedure

In order to proceed with the solution of the problem, it is necessary to determine the exit thermodynamic properties of the air streams through the matrix. The first step is to obtain the exit conditions for a single matrix element. A step procedure to obtain this may be outlined as

a) Assume the matrix temperature at the exit of an element $T(i,j+1) = T(i,j)$.

b) Evaluate the average surface temperature of the given element.

c) The average humidity ratio at the surface of the element is evaluated, according to equation (4-2) if the average surface temperature is below the dew point temperature of the entering air; if that is not the case, the average humidity ratio is identical to the humidity ratio of the entering air. In a similar manner, the average enthalpy of the air at the surface of the element is evaluated.

d) Substitution of the above values in equations (3-27) and (3-28) yields two values for the enthalpy, $h_\infty = h_\infty(i+1,j)$.

e) If the two enthalpies are not identical, within .04 percent, a new $T(i,j+1)$ is substituted and the process is repeated until both equations yield the same value of enthalpy, within the acceptable error.

Having obtained $T(i,j+1)$ and $h_\infty(i+1,j)$, the rest of the exit properties of the element may be calculated with the help of equations (3-23) through (3-26).

The next step is to assume a distribution of temperatures at the left edge of the hot side of the matrix; i.e., an assignment of the temperatures $T(1,1)$, $T(2,1)$ ...... $T(N_r,1)$ (see Figure 5). Since the entrance conditions of the hot air for the element (1,1) have been obtained, assuming the temperature $T(1,1)$ above and the initial entering condition of the hot air in the matrix, the procedure to obtain the exit conditions for the element (1,1) is similar to the one outlined in the preceding. Obviously, the exit condition of enthalpy for element (1,1) becomes the entering condition of the hot air for element (2,1). The procedure can be repeated to obtain the distribution of enthalpies along the first column of elements and the distribution of matrix temperatures for the right side of the same column of elements. In a similar fashion, the remaining columns of the hot side of the matrix are solved.

To solve for the cold sector side of the matrix, one needs only to adopt the procedure used for the hot sector side, noting that the temperature distribution on the left cold side of the matrix must equal the temperature distribution on the right hot side of the matrix, and that the first element to be calculated is the one at the left bottom of the cold side, where the entrance conditions are known. When the cold side of the matrix is solved, the reversal condition must be satisfied within 0.01 percent. This condition demands that

$$T_c(N_r + 1 - i,\ N_c + 1) = T_h(i,1)\ ; \qquad i + 1,2,3 \ldots N_r \ . \tag{4-5}$$

In the event that equation (4-5) is not satisfied, the temperature distribution originally assigned to the left edge of the hot side of the matrix is replaced by the calculated temperature distribution at the right edge of the cold side of the matrix. The procedure is repeated to eventually satisfy the reversal condition.

CHAPTER V

PRESENTATION AND DISCUSSION OF RESULTS

A Note on the Presentation of Results

To help attain a physical understanding of the results, all steady state property distributions are presented in matrix form, the latter being identical to the developed matrix of the rotary regenerator. Distributions for the hot and cold sides are represented in separate tables, each of which represents approximately one half of the developed matrix. Among the property distributions presented in the results are the temperature of the matrix, the enthalpy of air, the humidity ratio of air, and the mass rate of condensed water, as well as the states of entering and leaving hot and cold streams. Specific cases are examined for two air flow heat capacity rates, two matrix heat capacity rates, and two heat conductance ratios, the results being examined with respect to the number of heat transfer units of the rotary heat exchanger and heat exchanger effectiveness. A particular set of numerical information to illustrate the results of this study is shown in Table 1.

Property Distributions within the Matrix

Tables 2 and 3, respectively, show the distribution of enthalpies of the hot and cold air streams within the matrix. The top row of Table 2 and the bottom row of Table 3 represent the constant enthalpies of hot and cold air entering the matrix. As the hot stream passed down the

Table 1. Illustrative Set of Numerical Values

Input Parameters and Properties

Number of rows into which the matrix is divided: 10

$C_{min}/C_{max} = 0.7$

$C_r/C_{min} = 2$

NTUo = 8

Relative humidity of hot entering air = 60%

Temperature of hot entering air = 100°F

Enthalpy of hot entering air = 44.07 Btu/lbm

Relative humidity of cold entering air = 50%

Temperature of cold entering air = 80°F

Enthalpy of cold entering air = 23.48 Btu/lbm

Output Properties

Enthalpy of hot leaving air = 39.76 Btu/lbm

Enthalpy of cold leaving air = 28.06 Btu/lbm

Computer Time = 4.51 minutes

Table 2. Enthalpy of Air in the Hot Part of the Developed Matrix

44.07	44.07	44.07	44.07	44.07	44.07	44.07	44.07	44.07	44.07
43.44	43.56	43.72	43.77	43.79	43.85	43.94	43.97	43.97	43.97
43.08	43.13	43.31	43.36	43.46	43.53	43.60	43.72	43.76	43.78
42.65	42.78	42.85	43.00	43.10	43.19	43.27	43.37	43.44	43.48
42.21	42.39	42.43	42.60	42.67	42.82	42.91	43.02	43.10	43.16
41.79	41.90	42.00	42.19	42.25	42.36	42.53	42.59	42.73	42.82
41.33	41.44	41.56	41.70	41.81	41.91	42.05	42.15	42.26	42.38
40.77	40.89	41.07	41.15	41.32	41.45	41.57	41.69	41.81	41.92
40.08	40.61	40.39	40.58	40.74	40.88	41.01	41.14	41.32	41.39
38.09	39.61	40.17	40.42	40.62	40.79	40.94	40.44	40.62	40.81
36.41	38.13	39.32	39.98	40.36	40.61	40.80	40.68	40.62	40.74

NOTES: a) Hot air enters at top left.

b) Columns indicate angular positions along the matrix circumference at an interval of 20° each.

c) Rows indicate axial positions along the matrix length.

Table 3. Enthalpy of Air in the Cold Part of the Developed Matrix

30.11941	28.09440	28.03082	27.98095	27.89512	27.88261	27.77042	27.65736	27.64417	27.50429
29.92846	27.88260	27.77961	27.75253	27.60788	27.54742	27.45385	27.33955	27.30299	27.14836
29.59091	27.58000	27.47357	27.39103	27.25121	27.21777	27.08543	27.01155	26.93201	26.77775
29.25540	27.22675	27.08247	27.03956	26.90486	26.83170	26.74611	26.58013	26.50386	26.40630
28.89594	26.85779	26.72359	26.65156	26.56113	26.39365	26.30797	26.19351	26.07412	25.94614
28.51390	26.47197	26.38500	26.21412	26.11530	26.00741	25.85912	25.70920	25.59135	25.44549
28.13339	26.07680	25.93262	25.81934	25.64861	25.54083	25.32017	25.17512	25.02545	24.83532
27.98904	25.70717	25.56681	25.32165	25.07463	24.89963	24.68665	24.48729	24.34230	24.24949
28.71479	25.25908	24.84513	24.47966	24.24273	24.01622	23.90554	23.73759	23.66657	23.63707
33.30295	22.61549	22.74968	22.92937	22.99918	23.10912	23.13496	23.21864	23.26458	23.29309
23.48267	23.48267	23.48267	23.48267	23.48267	23.48267	23.48267	23.48267	23.48267	23.48267

NOTES: a) Cold air enters at lower left.

b) Columns indicate angular positions along the matrix circumference at an interval of 20° each.

c) Rows indicate axial positions along the matrix length.

passages in the matrix it delivers energy to the metal matrix elements, a process indicated by a decrease in enthalpy. In a similar fashion the cold stream entering at a lower level of enthalpy at the bottom of the cold part of the matrix primarily receives energy from the hotter metal matrix, this process resulting in an increase of enthalpy of the cold stream as it moves up through the matrix. The bottom row of Table 2 and the top row of Table 3, respectively, represent the enthalpies of the hot and cold streams leaving the matrix. Average values of these exit enthalpies are shown in Table 1.

Tables 4 and 5, respectively, show the distribution of temperature within the hot and cold sides of the matrix. The same information, for selected rows of the entire matrix, is shown graphically in Figure 7. The predominant variation of temperature is seen to be along the rows in these two tables, since these correspond to the rotation of the matrix about its axis. The last column of Table 4 also represents the first column of Table 5, since it represents the state of the matrix column leaving the hot domain and entering the cold domain. The trend, previously explained in connection with the discussion on enthalpy distribution, is visible in the temperature distribution as well; viz, a rise in matrix temperature due to energy received from the hot air stream, with a subsequent decrease in matrix temperature due to energy transferred to the cold stream. The last column of Table 5 is the input information for iteration of the property distributions. Ideally, this column should be identical to the first column of Table 4, the actual difference being the allowed truncation error in satisfying the so-called reversal condition.

Table 4. Temperature of the Hot Part of the Developed Matrix

96.52	97.20	97.74	98.12	98.44	98.75	98.98	99.12	99.23	99.33	99.43
95.22	95.62	96.08	96.52	96.95	97.31	97.66	98.02	98.28	98.50	98.71
93.63	94.09	94.47	94.97	95.35	95.73	96.10	96.47	96.84	97.19	97.50
91.98	92.45	92.87	93.32	93.75	94.21	94.61	94.99	95.37	95.73	96.07
90.15	90.60	91.12	91.58	92.02	92.48	92.97	93.39	93.85	94.24	94.60
88.16	88.66	89.15	89.63	90.16	90.63	91.12	91.63	92.10	92.60	93.08
85.84	86.44	87.04	87.56	88.14	88.66	89.15	89.65	90.14	90.63	91.12
83.20	83.93	84.26	84.98	85.60	86.23	86.84	87.44	88.03	88.56	89.12
80.55	82.58	83.62	83.86	84.05	84.21	84.35	84.48	85.23	85.97	86.59
79.25	80.95	82.46	83.32	83.76	84.02	84.21	84.36	84.14	84.18	84.30

NOTES: a) Hot air enters at top left.

b) Columns indicate angular positions along the matrix circumference at an interval of 20° each.

c) Rows indicate axial positions along the matrix length.

Table 5. Temperature of the Cold Part of the Developed Matrix

99.43	99.24	99.02	98.76	98.53	98.23	97.89	97.57	97.24	96.89	96.53
98.71	98.36	98.06	97.74	97.37	97.02	96.68	96.31	95.97	95.59	95.22
97.50	97.16	96.80	96.40	96.04	95.70	95.30	94.96	94.52	94.08	93.70
96.07	95.70	95.32	94.96	94.57	94.22	93.77	93.32	92.93	92.49	92.02
94.60	94.21	93.82	93.47	93.03	92.57	92.18	91.72	91.22	90.73	90.22
93.08	92.69	92.29	91.83	91.43	90.95	90.48	89.93	89.38	88.81	88.19
91.12	90.97	90.60	90.22	89.72	89.13	88.48	87.84	87.14	86.45	85.85
89.12	89.86	89.40	88.67	87.81	86.97	86.08	85.29	84.53	83.85	83.23
86.59	91.23	88.55	86.43	84.86	83.60	82.68	81.90	81.38	80.97	80.62
84.30	75.15	76.03	76.77	77.33	77.83	78.21	78.56	78.83	79.05	79.25

NOTES: a) Cold air enters at lower left.

b) Columns indicate angular positions along the matrix circumference at an interval of 20° each.

c) Rows indicate axial positions along the matrix length.

The distribution of humidity ratio of the hot and cold air is, respectively, shown in Tables 6 and 7. It is seen from Table 6 that, except for the bottom three rows, the humidity ratio is constant through the hot domain. This implies that condensation of water in the hot domain occurs only within the bottom three rows. The actual amount of condensation can be interpreted in terms of the decrease in humidity ratio of hot air along the three rows. On the other hand, only the first column of Table 7 indicates any change in the humidity ratio. In fact, this occurs only on the bottom element of the first column of Table 7. An account of this behavior might be provided by the carry-over of condensed water from the hot side to the cold side, a subsequent transfer of energy from this water to the relatively cooler entering air, and an eventual evaporation of all the carried water owing to heat absorbed from the matrix. There is no further increase in specific humidity of the first column of the cold side.

A qualitative verification of the explanation regarding carry-over can be sought by examining Tables 8 and 9, which respectively represent the distribution of the rate of condensed water within the hot and cold sides of the matrix. It is clearly seen from Table 8 that condensation does occur within the bottom three rows and also that the rate of condensation increases to a maximum along the rows, followed by a reevaporation of a portion of the condensate, resulting in an apparent display of a reduced condensation. The portion of condensate that does not get reevaporated on the hot side is carried over to the cold side as explained previously.

Table 6. Specific Humidity of the Hot Part of the Developed Matrix

.02511	.02511	.02511	.02511	.02511	.02511	.02511	.02511	.02511	.02511
.02511	.02511	.02511	.02511	.02511	.02511	.02511	.02511	.02511	.02511
.02511	.02511	.02511	.02511	.02511	.02511	.02511	.02511	.02511	.02511
.02511	.02511	.02511	.02511	.02511	.02511	.02511	.02511	.02511	.02511
.02511	.02511	.02511	.02511	.02511	.02511	.02511	.02511	.02511	.02511
.02511	.02511	.02511	.02511	.02511	.02511	.02511	.02511	.02511	.02511
.02511	.02511	.02511	.02511	.02511	.02511	.02511	.02511	.02511	.02511
.02511	.02511	.02511	.02511	.02511	.02511	.02511	.02511	.02511	.02511
.02510	.02513	.02511	.02511	.02511	.02511	.02511	.02511	.02511	.02511
.02377	.02478	.02522	.02536	.02548	.02559	.02557	.02511	.02511	.02511
.02260	.02380	.02466	.02512	.02539	.02556	.02568	.02557	.02551	.02556

NOTES: a) Hot air enters at top left.

b) Columns indicate angular positions along the matrix circumference at an interval of 20° each.

c) Rows indicate axial positions along the matrix length.

Table 7. Specific Humidity of the Cold Part of the Developed Matrix

.01270	.01092	.01092	.01092	.01092	.01092	.01092	.01092	.01092	.01092
.01270	.01092	.01092	.01092	.01092	.01092	.01092	.01092	.01092	.01092
.01270	.01092	.01092	.01092	.01092	.01092	.01092	.01092	.01092	.01092
.01270	.01092	.01092	.01092	.01092	.01092	.01092	.01092	.01092	.01092
.01270	.01092	.01092	.01092	.01092	.01092	.01092	.01092	.01092	.01092
.01270	.01092	.01092	.01092	.01092	.01092	.01092	.01092	.01092	.01092
.01270	.01092	.01092	.01092	.01092	.01092	.01092	.01092	.01092	.01092
.01270	.01092	.01092	.01092	.01092	.01092	.01092	.01092	.01092	.01092
.01270	.01092	.01092	.01092	.01092	.01092	.01092	.01092	.01092	.01092
.01270	.01092	.01092	.01092	.01092	.01092	.01092	.01092	.01092	.01092
.01092	.01092	.01092	.01092	.01092	.01092	.01092	.01092	.01092	.01092

NOTES: a) Cold air enters at lower left.

b) Columns indicate angular positions along the matrix circumference at an interval of 20° each.

c) Rows indicate axial positions along the matrix length.

Table 8. Mass Rate of Condensed Water on Hot Part of the Developed Matrix

.00000	.00000	.00000	.00000	.00000	.00000	.00000	.00000	.00000	.00000	.00000
.00000	.00000	.00000	.00000	.00000	.00000	.00000	.00000	.00000	.00000	.00000
.00000	.00000	.00000	.00000	.00000	.00000	.00000	.00000	.00000	.00000	.00000
.00000	.00000	.00000	.00000	.00000	.00000	.00000	.00000	.00000	.00000	.00000
.00000	.00000	.00000	.00000	.00000	.00000	.00000	.00000	.00000	.00000	.00000
.00000	.00000	.00000	.00000	.00000	.00000	.00000	.00000	.00000	.00000	.00000
.00000	.00000	.00000	.00000	.00000	.00000	.00000	.00000	.00000	.00000	.00000
.00000	.00239	.00000	.00000	.00000	.00000	.00000	.00000	.00000	.00000	.00000
.00000	.19879	.25049	.23480	.19701	.14098	.06940	.00000	.00000	.00000	.00000
.00000	.17556	.32300	.40681	.44266	.45721	.46106	.44533	.37684	.31768	.25023

NOTES: a) Hot air enters at top left.

b) Columns indicate angular positions along the matrix circumference at an interval of 20° each.

c) Rows indicate axial positions along the matrix length.

Table 9. Mass Rate of Condensed Water on Cold Part of the Developed Matrix

.00000	.00000	.00000	.00000	.00000	.00000	.00000	.00000	.00000	.00000	.00000
.00000	.00000	.00000	.00000	.00000	.00000	.00000	.00000	.00000	.00000	.00000
.00000	.00000	.00000	.00000	.00000	.00000	.00000	.00000	.00000	.00000	.00000
.00000	.00000	.00000	.00000	.00000	.00000	.00000	.00000	.00000	.00000	.00000
.00000	.00000	.00000	.00000	.00000	.00000	.00000	.00000	.00000	.00000	.00000
.00000	.00000	.00000	.00000	.00000	.00000	.00000	.00000	.00000	.00000	.00000
.00000	.00000	.00000	.00000	.00000	.00000	.00000	.00000	.00000	.00000	.00000
.00000	.00000	.00000	.00000	.00000	.00000	.00000	.00000	.00000	.00000	.00000
.00000	.00000	.00000	.00000	.00000	.00000	.00000	.00000	.00000	.00000	.00000
.25023	.00000	.00000	.00000	.00000	.00000	.00000	.00000	.00000	.00000	.00000

NOTES: a) Cold air enters at lower left.

b) Columns indicate angular positions along the matrix circumference at an interval of 20° each.

c) Rows indicate axial positions along the matrix length.

Parametric Considerations of the Regenerator Performance

Figures 8 through 11 show the performance curves of the rotary regenerator under the influence of several parameters. Each of these curves was obtained by a careful examination of the data from several sets of eight tables similar to those discussed previously. The rotary regenerator effectiveness and the number of transfer units (NTUo) are the basic variables in these curves, plotted for two values of the ratio of minimum to maximum heat capacity rates, C_{min}/C_{max}, two values of the ratio of rotor heat capacity rate to the minimum heat capacity rate of air, C_r/C_{min}, and two values of the ratio of effective conductance (hA)*.

It is recognized that the number of transfer units, NTU, expresses the "heat transfer size" of a heat exchanger configuration. As such, it is to be expected that the higher value of NTUo should correspond to a greater heat transfer rate, both from the hot air to the matrix as well as from the matrix to the cold air. Such a trend is seen in Figure 8. Further, an examination of Tables 10 and 11, respectively representing the enthalpy distribution for the hot domain for NTUo = 5 and NTUo = 8, and an examination of Tables 12 and 13, respectively representing the cold domain enthalpy distribution for NTUo = 5 and NTUo = 8, confirm the expectation regarding the hot and cold domain heat transfer rates. Moreover, an examination of the distribution of condensing rates for NTUo = 5 and NTUo = 8, respectively shown in Tables 14 and 15, indicates a higher condensation rate for the higher NTUo case, an observation consistent with the greater heat transfer rate mentioned earlier. Similar observations regarding the influence of NTUo can be made from Figures 9, 10, and 11.

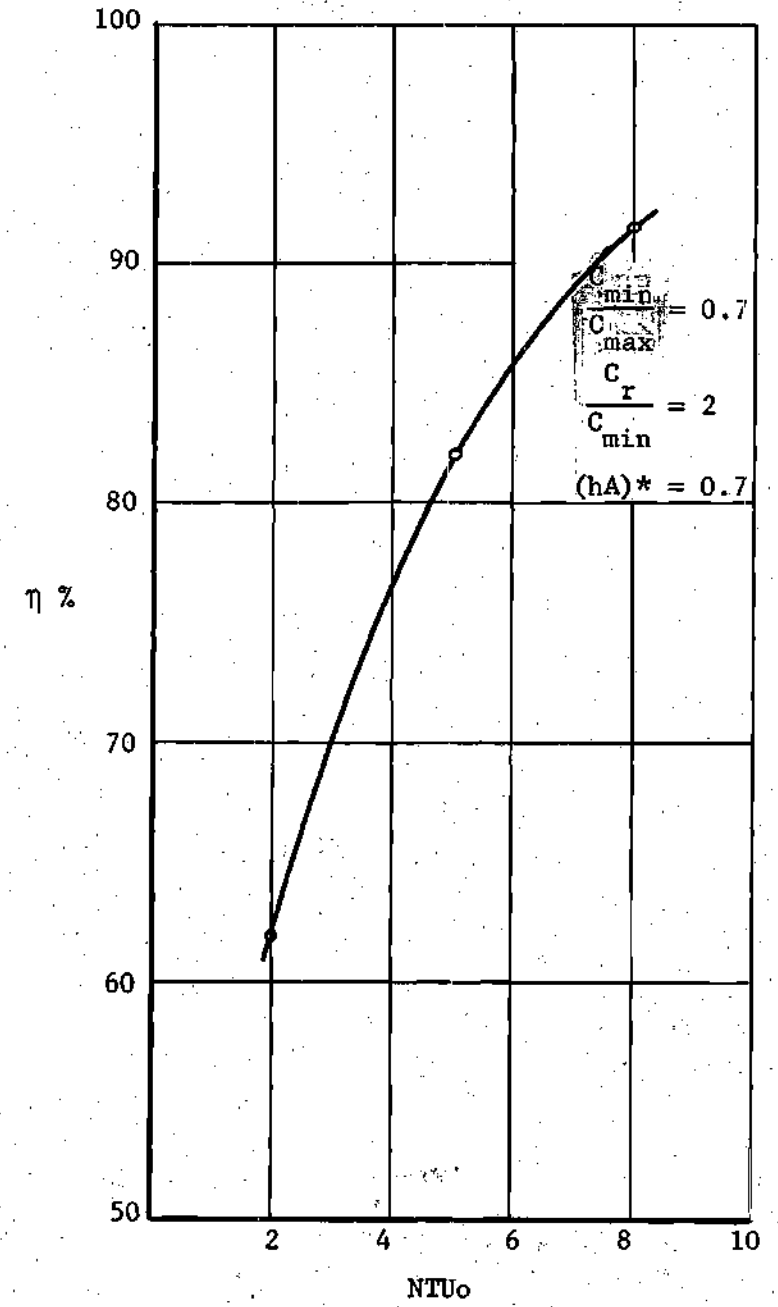

Figure 8. Effectiveness versus NTUo for $C_{min}/C_{max} = 0.7$, $C_r/C_{min} = 2$, $(hA)^* = 0.7$

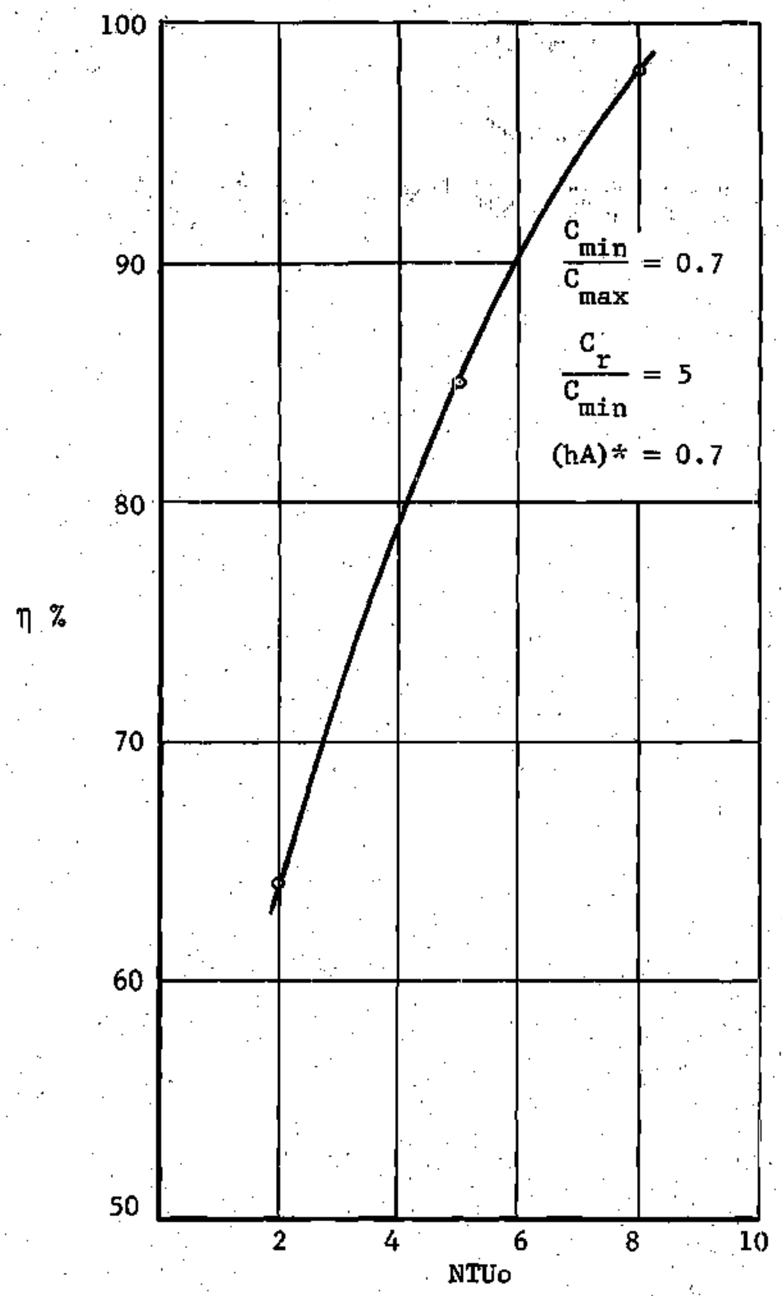

Figure 9. Effectiveness versus NTUo for $C_{min}/C_{max} = 0.7$, $C_r/C_{min} = 5$, $(hA)^* = 0.7$

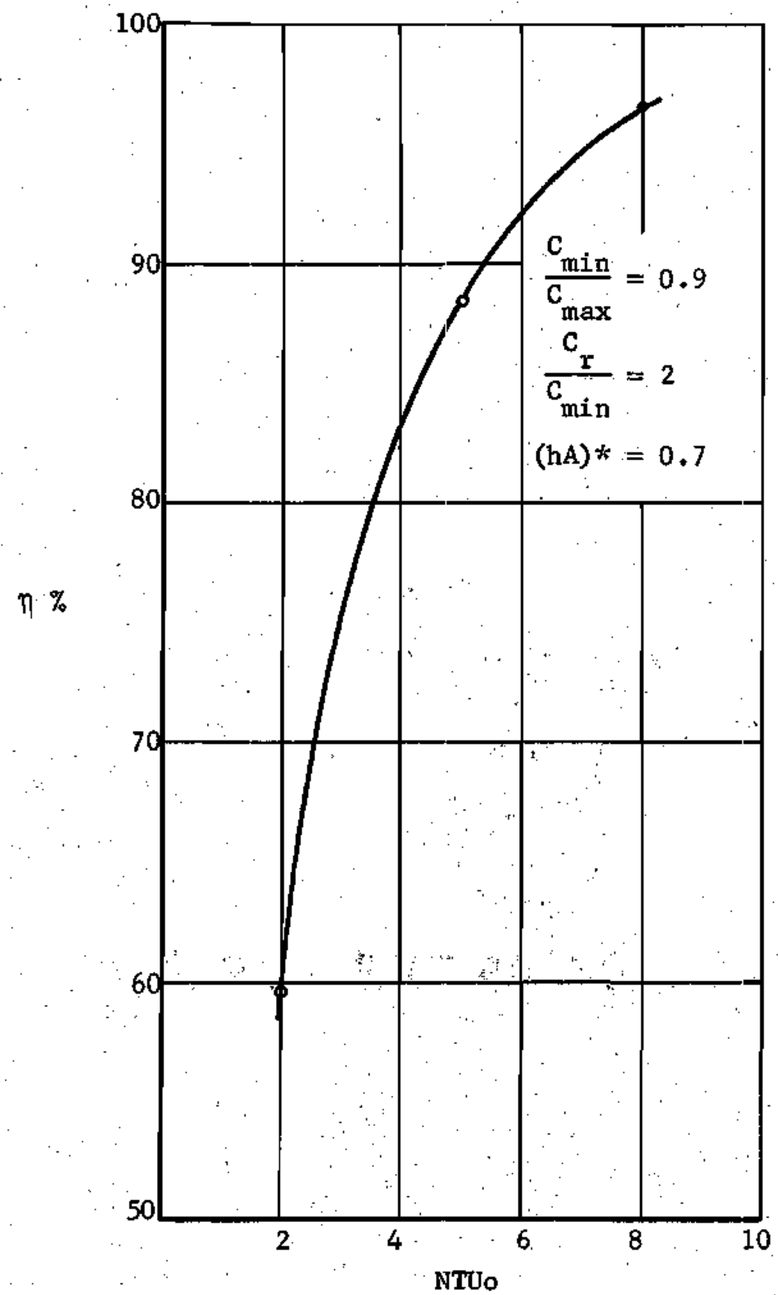

Figure 10. Effectiveness versus NTUo for $C_{min}/C_{max} = 0.9$, $C_r/C_{min} = 2$, $(hA)^* = 0.7$

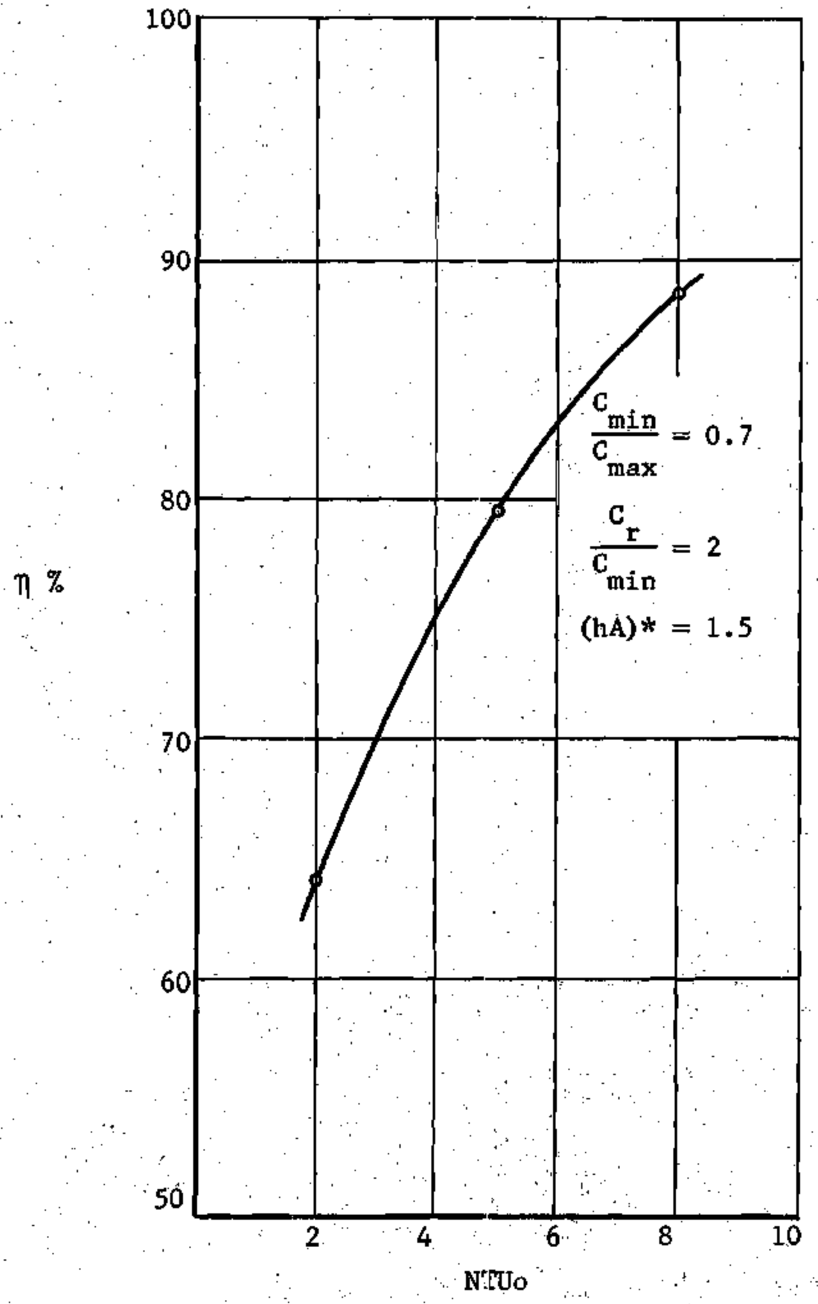

Figure 11. Effectiveness versus NTUo for $C_{min}/C_{max} = 0.7$, $C_r/C_{min} = 2$, $(hA)^* = 1.5$

Table 10. Enthalpy of Air in the Hot Part of the Developed Matrix

44.07	44.07	44.07	44.07	44.07	44.07	44.07	44.07	44.07	44.07	44.07
43.60	43.66	43.70	43.74	43.78	43.80	43.84	43.86	43.87	43.91	43.94
43.18	43.28	43.35	43.41	43.46	43.53	43.55	43.61	43.64	43.69	43.72
42.80	42.91	43.00	43.07	43.13	43.20	43.27	43.31	43.38	43.45	43.49
42.43	42.55	42.64	42.72	42.79	42.86	42.98	43.01	43.09	43.16	43.23
42.08	42.19	42.29	42.38	42.45	42.53	42.63	42.68	42.77	42.86	42.92
41.70	41.82	41.93	42.02	42.10	42.18	42.28	42.34	42.43	42.51	42.58
41.31	41.44	41.52	41.64	41.74	41.83	41.92	42.00	42.08	42.17	42.24
40.92	41.02	41.14	41.27	41.34	41.45	41.55	41.64	41.73	41.82	41.90
40.27	40.61	40.86	40.80	40.89	41.04	41.13	41.23	41.33	41.44	41.52
39.08	39.77	40.28	40.48	40.68	40.88	41.01	41.14	41.26	40.98	41.07
37.76	38.71	39.46	39.92	40.28	40.58	40.80	40.98	41.13	41.01	41.07

NOTES: a) Hot air enters at top left. b) Columns indicate angular positions along the matrix circumference at an interval of 20° each. c) Rows indicate axial positions along the matrix length. d) NTUo = 5.

e) $\frac{C_{min}}{C_{max}} = 0.7$.

f) $\frac{C_r}{C_{min}} = 2$.

Table 11. Enthalpy of Air in the Hot Part of the Developed Matrix

44.07	44.07	44.07	44.07	44.07	44.07	44.07	44.07	44.07	44.07	44.07
43.55	43.63	43.67	43.74	43.77	43.83	43.86	43.90	43.92	43.95	43.97
43.15	43.21	43.31	43.40	43.45	43.51	43.60	43.66	43.70	43.73	43.76
42.73	42.84	42.95	43.04	43.12	43.18	43.26	43.33	43.43	43.45	43.52
42.33	42.46	42.58	42.69	42.77	42.84	42.92	43.00	43.08	43.13	43.24
41.95	42.09	42.21	42.27	42.39	42.49	42.58	42.66	42.74	42.80	42.89
41.54	41.69	41.78	41.90	41.97	42.10	42.21	42.26	42.37	42.46	42.55
41.10	41.23	41.33	41.49	41.55	41.68	41.80	41.90	41.95	42.08	42.19
40.58	40.74	40.84	40.97	41.08	41.22	41.34	41.44	41.52	41.68	41.76
39.34	40.09	40.50	40.77	40.96	40.66	40.78	40.94	41.01	41.19	41.30
37.71	38.95	39.77	40.31	40.67	40.67	40.75	40.87	40.97	41.11	41.24
36.65	37.86	38.87	39.64	40.19	40.45	40.62	40.76	40.88	41.02	41.15

NOTES: a) Hot air enters at top left. b) Columns indicate angular positions along the matrix circumference at an interval of 20° each. c) Rows indicate axial positions along the matrix length. d) NTUo = 8.

e) $\frac{C_{min}}{C_{max}} = 0.7$.

f) $\frac{C_r}{C_{min}} = 2$.

Table 12. Enthalpy of Air in the Cold Part of the Developed Matrix

29.45825	27.86223	27.76954	27.66749	27.59201	27.52295	27.43368	27.40775	27.32129	27.22036	27.11858
29.18750	27.58033	27.47554	27.37006	27.32560	27.26581	27.14886	27.06038	27.03686	26.91804	26.81646
28.90315	27.28077	27.16470	27.06533	27.02324	26.94409	26.82769	26.77459	26.69361	26.59156	26.51288
28.59305	26.96096	26.84051	26.76352	26.72457	26.60011	26.50301	26.45880	26.34737	26.28732	26.16237
28.25006	26.62528	26.50947	26.40834	26.36159	26.26391	26.20673	26.08468	26.02898	25.88653	25.82519
27.89745	26.29531	26.18672	26.14549	26.02368	25.96477	25.81399	25.74557	25.63904	25.52634	25.41951
27.60787	25.99359	25.87276	25.77500	25.68906	25.56475	25.44117	25.33888	25.24558	25.13036	24.95646
27.39280	25.68124	25.54342	25.47196	25.25934	25.14908	25.02887	24.88877	24.78294	24.65372	24.54195
27.45120	25.40597	25.20073	25.04272	24.81219	24.66945	24.52936	24.36809	24.30284	24.15949	24.06117
28.49370	24.85164	24.58596	24.33849	24.15263	23.98628	23.84920	23.80877	23.73311	23.62923	23.59491
32.68224	22.84928	22.91016	23.01166	23.07344	23.17457	23.23777	23.27228	23.29564	23.30728	23.37800
23.48267	23.48267	23.48267	23.48267	23.48267	23.48267	23.48267	23.48267	23.48267	23.48267	23.48267

NOTES: a) Cold air enters at lower left. b) Columns indicate angular positions along the matrix circumference at an interval of 20° each. c) Rows indicate axial positions along the matrix length. d) NTUo = 0.7.

e) $\frac{C_{min}}{C_{max}} = 0.7$.

f) $\frac{C_r}{C_{min}} = 2$.

Table 13. Enthalpy of Air in the Cold Part of the Developed Matrix

30.45182	28.11539	28.03641	27.95771	27.87398	27.79877	27.73940	27.65854	27.61307	27.54977	27.42874
30.20107	27.83480	27.76524	27.68866	27.59093	27.55092	27.48971	27.36777	27.30365	27.21263	27.09774
29.88108	27.52278	27.52500	27.39582	27.29329	27.26770	27.13625	27.05463	26.96916	26.83408	26.80135
29.55663	27.20852	27.18998	27.05239	27.01559	26.86822	26.82724	26.67144	26.62865	26.47755	26.43355
29.28877	26.88091	26.84182	26.69012	26.64802	26.49643	26.44832	26.29494	26.24841	26.10553	26.05517
28.88581	26.52401	26.46705	26.31705	26.27287	26.11565	26.06696	25.91764	25.85878	25.76412	25.64125
28.50482	26.11310	26.08371	25.94612	25.89448	25.73226	25.67064	25.56466	25.42888	25.29278	25.13601
28.09480	25.78874	25.70064	25.60915	25.47011	25.36154	25.24334	25.06767	24.91656	24.78236	24.56542
27.70017	25.51615	25.41119	25.32349	25.05936	24.84907	24.63279	24.37675	24.22173	24.12121	23.94906
28.07446	25.68039	25.01629	24.54704	24.15609	23.87365	23.70330	23.59164	23.57637	23.51112	23.41061
34.69885	22.29870	22.52964	22.72435	22.86099	23.00829	23.08641	23.20763	23.26562	23.29726	23.31057
23.48267	23.48267	23.48267	23.48267	23.48267	23.48267	23.48267	23.48267	23.48267	23.48267	23.48267

NOTES: a) Cold air enters at lower left. b) Columns indicate angular positions along the matrix circumference at an interval of 20° each. c) Rows indicate axial positions along the matrix length. d) NTUo = 8.

e) $\frac{C_{min}}{C_{max}} = 0.7$.

f) $\frac{C_r}{C_{min}} = 2$.

Table 14. Mass Rate of Condensed Water on the Hot Part of the Developed Matrix

.00000	.00000	.00000	.00000	.00000	.00000	.00000	.00000	.00000	.00000	.00000	.00000
.00000	.00000	.00000	.00000	.00000	.00000	.00000	.00000	.00000	.00000	.00000	.00000
.00000	.00000	.00000	.00000	.00000	.00000	.00000	.00000	.00000	.00000	.00000	.00000
.00000	.00000	.00000	.00000	.00000	.00000	.00000	.00000	.00000	.00000	.00000	.00000
.00000	.00000	.00000	.00000	.00000	.00000	.00000	.00000	.00000	.00000	.00000	.00000
.00000	.00000	.00000	.00000	.00000	.00000	.00000	.00000	.00000	.00000	.00000	.00000
.00000	.00000	.00000	.00000	.00000	.00000	.00000	.00000	.00000	.00000	.00000	.00000
.00000	.00000	.00000	.00000	.00000	.00000	.00000	.00000	.00000	.00000	.00000	.00000
.00000	.02285	.01868	.00000	.00000	.00000	.00000	.00000	.00000	.00000	.00000	.00000
.00000	.09221	.14799	.17510	.17121	.15282	.12368	.08615	.04189	.00000	.00000	.00000
.00000	.11444	.20180	.26362	.29757	.31384	.31677	.30953	.29482	.27097	.22584	.18004

NOTES: a) Hot air enters at top left. b) Columns indicate angular positions along the matrix circumference at an interval of 20° each. c) Rows indicate axial positions along the matrix length. d) NTUo = 5.

e) $\frac{C_{min}}{C_{max}} = 0.7$.

f) $\frac{C_r}{C_{min}} = 2$.

Table 15. Mass Rate of Condensed Water on the Hot Part of the Developed Matrix

.00000	.00000	.00000	.00000	.00000	.00000	.00000	.00000	.00000	.00000	.00000
.00000	.00000	.00000	.00000	.00000	.00000	.00000	.00000	.00000	.00000	.00000
.00000	.00000	.00000	.00000	.00000	.00000	.00000	.00000	.00000	.00000	.00000
.00000	.00000	.00000	.00000	.00000	.00000	.00000	.00000	.00000	.00000	.00000
.00000	.00000	.00000	.00000	.00000	.00000	.00000	.00000	.00000	.00000	.00000
.00000	.00000	.00000	.00000	.00000	.00000	.00000	.00000	.00000	.00000	.00000
.00000	.00000	.00000	.00000	.00000	.00000	.00000	.00000	.00000	.00000	.00000
.00000	.00000	.00000	.00000	.00000	.00000	.00000	.00000	.00000	.00000	.00000
.00000	.08322	.10053	.08149	.04122	.00000	.00000	.00000	.00000	.00000	.00000
.00000	.14235	.23367	.28334	.30393	.29742	.25453	.20891	.15749	.09930	.03388
.00000	.09666	.19431	.27310	.32872	.36100	.36540	.35842	.34565	.32913	.30938

NOTES: a) Hot air enters at top left. b) Columns indicate angular positions along the matrix circumference at an interval of 20° each. c) Rows indicate axial positions along the matrix length. d) NTUo = 8.

e) $\frac{C_{min}}{C_{max}} = 0.7$.

f) $\frac{C_r}{C_{min}} = 2$.

A very interesting observation regarding the influence of condensation on the rotary heat exchanger effectiveness can be made on the basis of the preceding discussion on the role played by NTUo in the heat transfer process. It appears that the start of cold air humidification, which might prove to be a critical design condition in applying the RHE to such systems where it is to be avoided, can be identified as a point on each of the NTUo - Effectiveness curves for a given set of such parameters as C_{min}/C_{max}, C_r/C_{min}, and (hA)*. In other words, although the effectiveness shows an apparent increase due to the cold air humidification, the need to avoid the latter puts an upper limit on the former. Figure 12 shows qualitatively how such design information might appear on the Effectiveness versus NTUo curve for prescribed states of entering air streams. That such information was not obtained in this investigation due to its previously stated limited scope, does not preclude a further exploration of the numerical model developed herein just to obtain such data.

Figure 13 shows the influence of the parameter C_{min}/C_{max} on the RHE effectiveness. It is seen that, for the case of a higher value of the heat capacity rate ratio, the effectiveness is higher, both for NTUo = 5 and for NTUo = 8. A possible explanation for such a trend can be provided by first observing that a higher value of C_{min}/C_{max} amounts to a higher flow rate of cold air in this investigation. As a result, the average temperature distribution within the matrix is at a lower level than that for the case of $C_{min}/C_{max} = 0.7$. The consequence of this is that, for the higher average temperature distribution, all the condensate

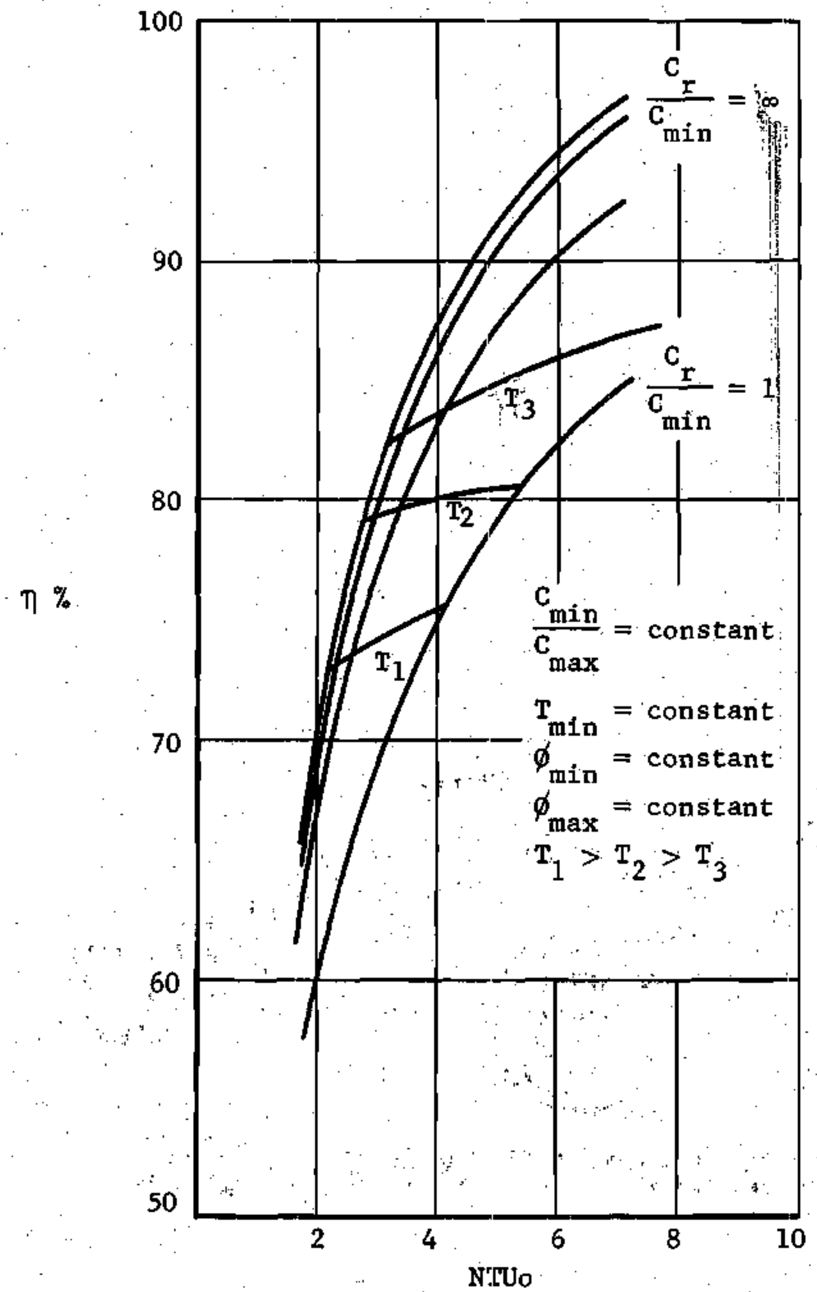

Figure 12. Qualitative Sketch of the Influence of Humidity

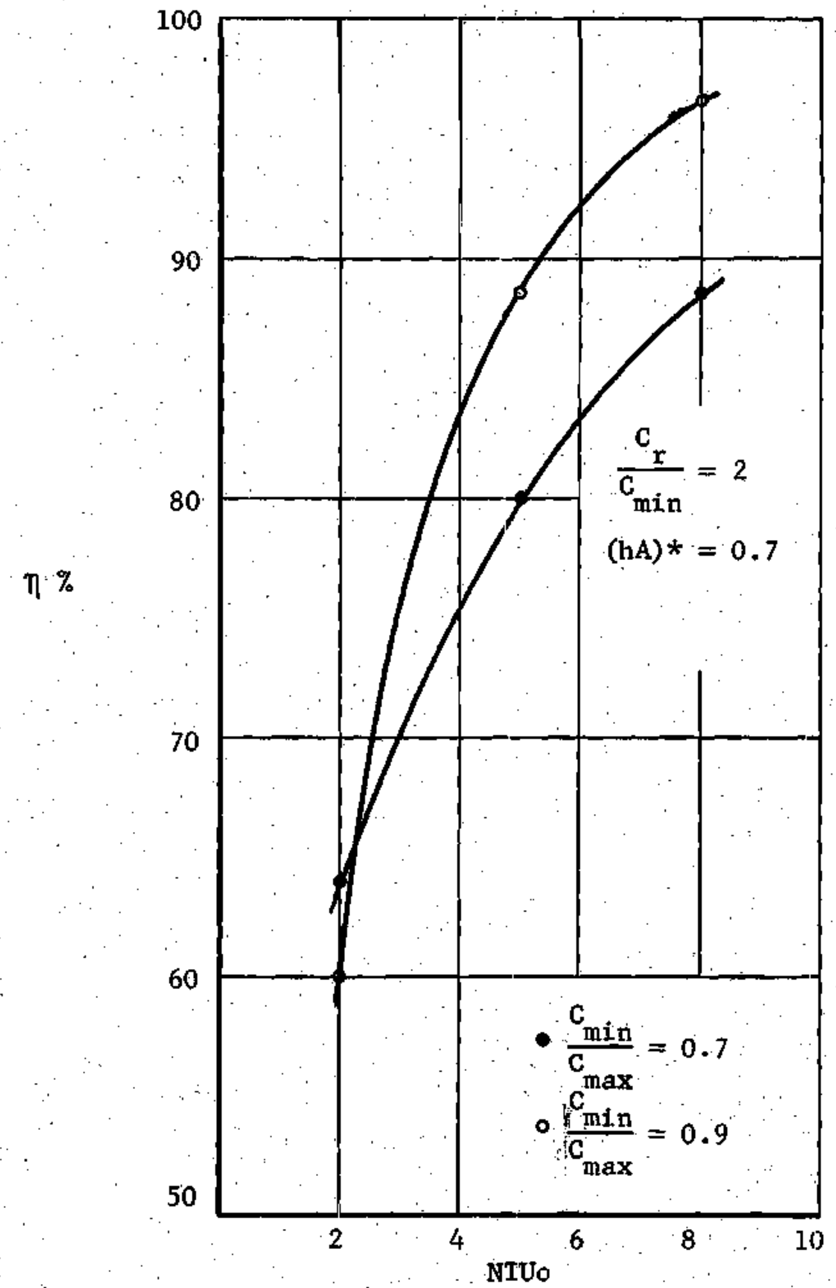

Figure 13. Influence of the Parameter C_{min}/C_{max} on the RHE Performance

in the hot domain is reevaporated prior to reaching the cold side. Such is not the case for the lower average temperature distribution; rather, there is a carry-over of condensate to the cold side. This condensate being at a higher temperature than the temperature of the incoming cold air allows a greater heat transfer to the latter. Although this influence is limited to only the first column of elements on the cold side (due to immediate reevaporation of condensate due to heat transfer from the matrix), the end result is a slight increase in regenerator effectiveness.

Figure 14 shows the influence of C_r/C_{min} on the regenerator performance. It is seen that, at a higher value of this parameter, the effectiveness improves. This trend has been previously observed by other investigators and has been explained on the basis that, at a higher heat capacity rate of the matrix, its performance approaches that of a non-rotating conventional counterflow exchanger.

The influence of (hA)*, although reported by other investigators to be negligible for the range of variation considered in this study, seems to be slightly in variance with other studies, as shown in Figure 15. It is likely that this is more a consequence of computational errors involved with the present model and the resultant truncation error than it is an indication of a physical mechanism.

Figure 16 shows the influence of increasing the number of matrix elements on the effectiveness of the regenerator. That this influence is extremely small is a proper justification for extrapolating the results to the case of a very large number of elements.

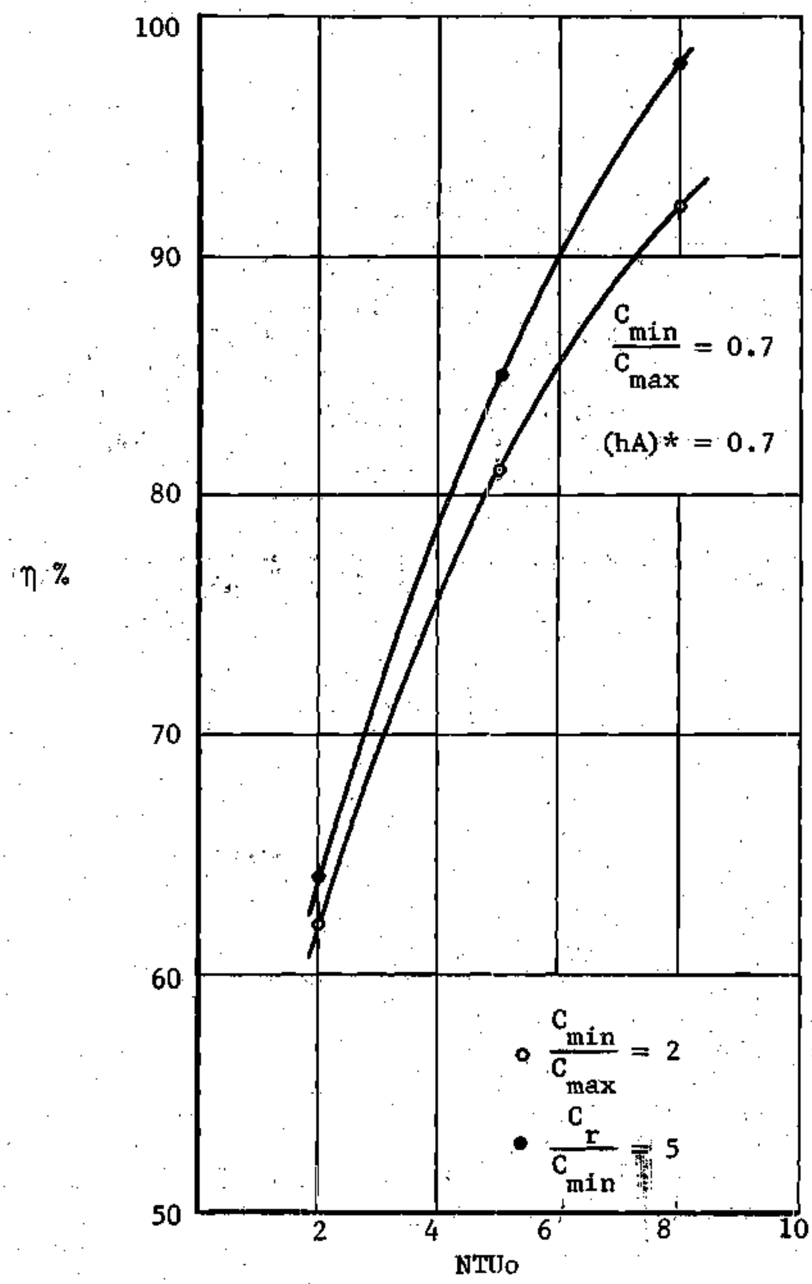

Figure 14. Influence of the Parameter C_r/C_{min} on the RHE Performance

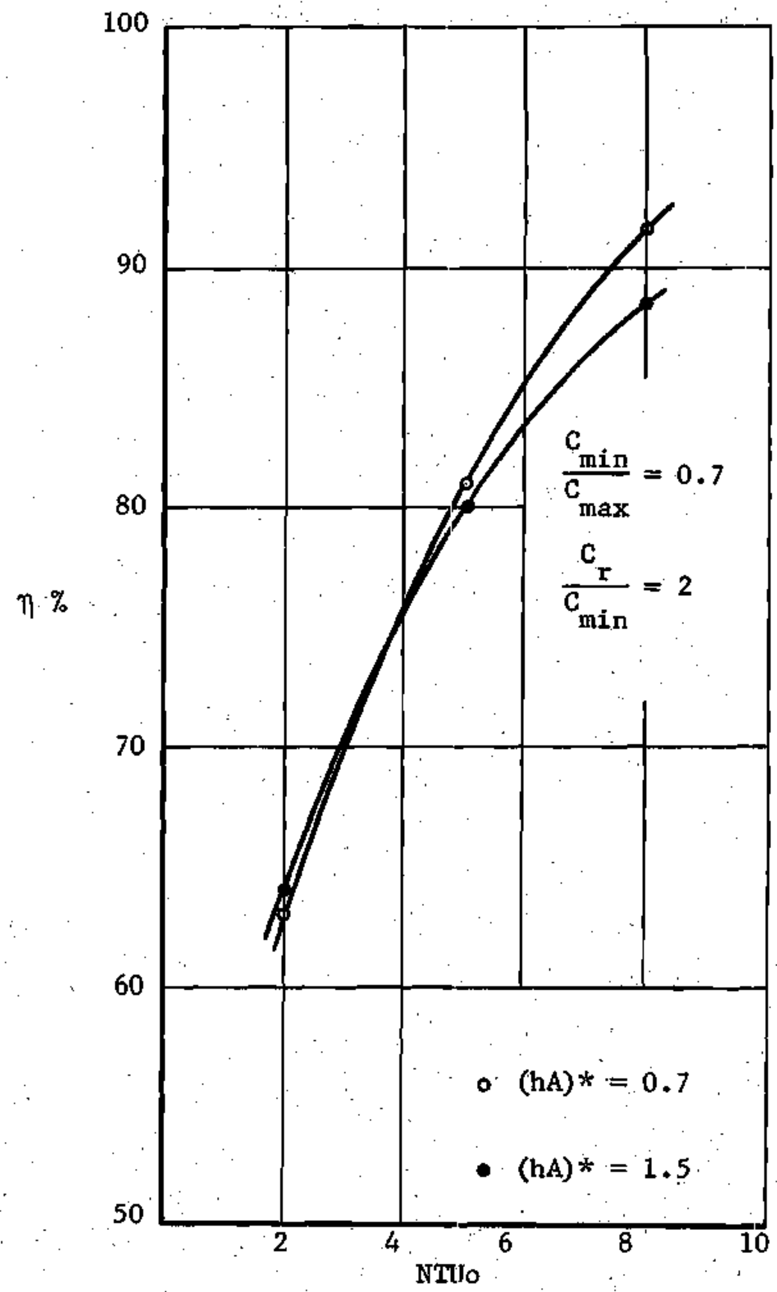

Figure 15. Influence of the Parameter (hA)* on the RHE Performance

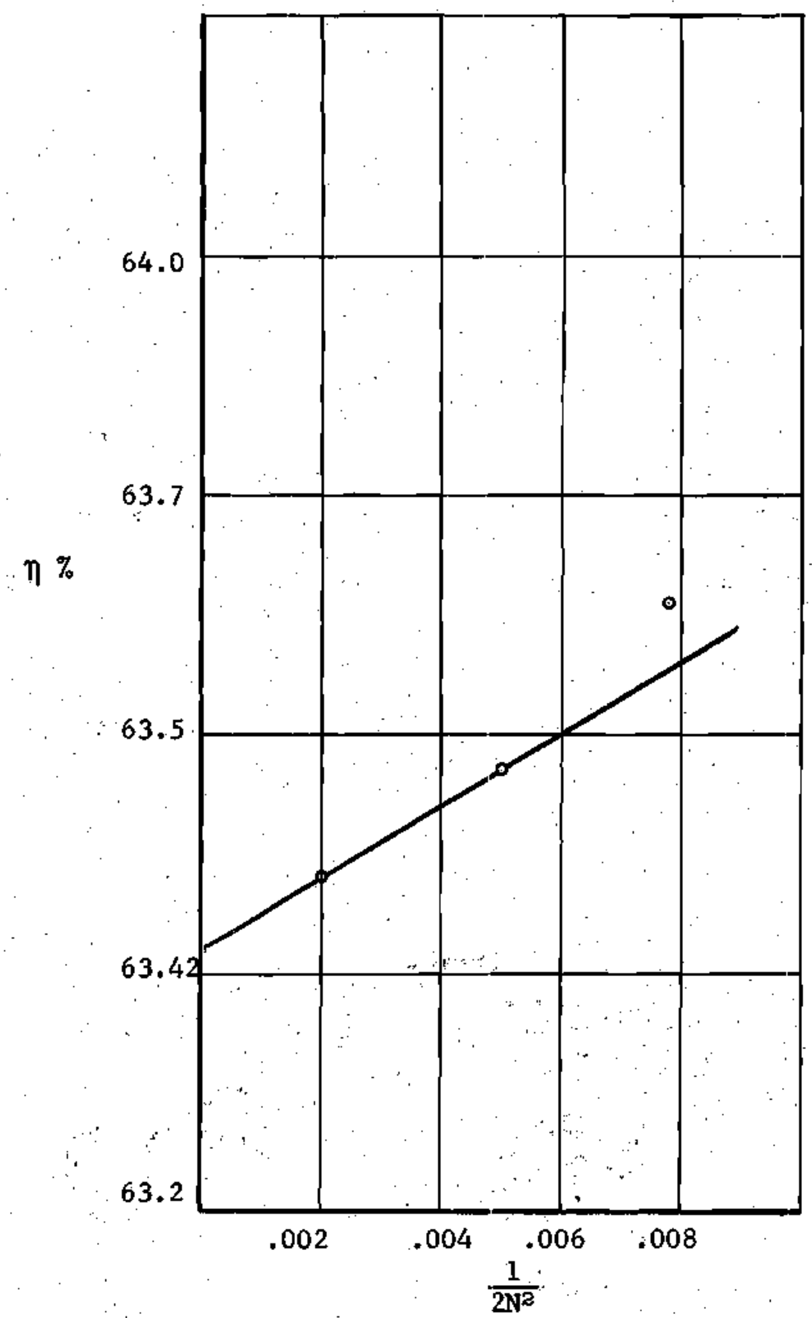

Figure 16. Influence of the Number of Elements on the RHE Performance

CHAPTER VI

CONCLUSIONS AND RECOMMENDATIONS

The research reported in this investigation has demonstrated that

i) It is feasible to examine rotary heat exchanger performance, with at least one condensing fluid stream through it, by the numerical technique developed in this work.

ii) Although an apparent increase in the rotary heat exchanger effectiveness occurs as a result of cold air humidification caused by a carry-over of condensate from the hot domain of the rotor matrix, the need to avoid humidification of cold air in certain applications puts an upper limit on the effectiveness of the heat exchanger.

For future investigations on the subject, it is suggested that

i) Emphasis be placed on examining in more detail the influence of both the heat capacity rate parameters considered in this investigation, with particular reference to the quantitative definition of the condensate carry-over conditions;

ii) For wider application of the numerical technique developed in this work, efforts be made to examine the influence of different entering gas stream states.

iii) A significantly large number of elements of the matrix be considered with truncation errors of computation limited to an order of magnitude smaller than those utilized in this work.

APPENDIX I

DERIVATION OF EQUATIONS (3-27) AND (3-28)

a) Derivation of Equation (3-27)

From Equation (3-23) and equation (3-20), we have

$$\dot{m}_w(i,j+1) = \frac{\dot{m}_a}{N}\left[W(i,j) - W(i+i,j)\right] + \dot{m}_w(i,j). \quad \text{(A-1)}$$

Let $$\dot{Q} = \frac{\dot{m}_a}{N}\left[h_\infty(i,j) - h_\infty(i+1,j)\right]. \quad \text{(A-2)}$$

Incorporating Equations (A-1) and (A-2) into Equation (3-21) yields

$$\dot{Q} = \frac{m_a}{N}\left[W(i,j) - W(i+1,j)\right] C_{pw}\ T(i,j+1) + \left[\dot{m}_w(i,j)\ C_{pw} + \frac{\dot{m}_r}{N}\ C_{pr}\right]\left[T(i,j+1) - T(i,j)\right] - \frac{kA_d}{2L}\left[(T(i-1,j) + T(i-1,j+1)) - 2(T(i,j) + T(i,j+1)) + (T(i+1,j) + T(i+1,j+1))\right]. \quad \text{(A-3)}$$

From Equation (3-24)

$$W(i+1,j) = \left[\frac{\dot{m}_a - \frac{fAv}{2C_{pm}\ N}}{\dot{m}_a + \frac{fAv}{2C_{pm}\ N}}\right] W(i,j) + \left[\frac{\frac{fA}{2C_{pm}\ N}}{\dot{m}_a + \frac{fAv}{2C_{pm}\ N}}\right] 2\ W_{savg}(i,j). \quad \text{(A-4)}$$

For simplification let

$$\frac{fA}{2\dot{m}_a C_{pm} N} = \frac{B}{N} = \frac{NTU}{2N} \ . \qquad \text{(A-5)}$$

Equation (A-4) can now be rewritten as

$$W(i+1,j) = \frac{N-B}{N+B} W(i,j) + \frac{2B}{N+B} W_{savg}(i,j) \ . \qquad \text{(A-6)}$$

Incorporation of Equation (A-6) into Equation (A-3) yields

$$= \frac{\dot{m}_a}{N} \left[\left(1 - \frac{N-B}{N+B}\right) W(i,j) - \frac{2B}{N+B} W_{savg}(i,j)\right] C_{pw} \ T(i,j+1) + \qquad \text{(A-7)}$$

$$\left[m_w(i,j) \ C_{pw} + \frac{m_r \ C_{pr}}{N}\right]\left[T(i,j+1) - T(i,j)\right] -$$

$$\dot{m}_a \ HC84 \left[(T(i-1,j) + T(i-1,j+1)) - 2(T(i,j) + T(i,j+1)) +\right.$$

$$\left.(T(i+1,j) + T(i+1,j+1))\right] ,$$

where $HC84 = \frac{kA}{2\dot{m}_a L}$; (A-8)

Finally combining Equations (A-7) and (A-8), one obtains

$$h_\infty(i+1,j) = h_\infty(i,j) - \frac{2B}{N+B}\left[W(i,j) - W_{savg}\right] C_{pw} \ T(i,j+1) - \qquad \text{(A-9)}$$

(Continued)

$$\left[\frac{\dot{m}_w(i,j)\ C_{pw}}{\frac{\dot{m}_a}{N}} + \frac{\dot{m}_r\ C_{pr}}{\dot{m}_a}\right]\left[T(i,j+1) - T(i,j)\right] - HC84\ N\left[(T(i-1,j) + T(i-1,j+1)) - 2(T(i,j) + T(i,j+1)) + (T(i+1,j) + T(i+1,j+1))\right].$$

If we incorporate Equations (3-29), (3-30), and (3-31) into Equation (A-9), we will have the resulting Equation (3-27).

b) Derivation of Equation (3-28)

From Equation (3-22) we have

$$h_\infty(i+1,j) = \frac{N-B}{N+B}\, h_\infty(i,j) + \frac{2B}{N+B}\, h_{savg}(i,j)\ . \tag{A-10}$$

Adding and subtracting $\frac{2B}{N+B}\, h_\infty(i,j)$,

$$h_\infty(i+1,j) = h_\infty(i,j) + HC81\ (h_{savg}(i,j) - h_\infty(i,j))\ , \tag{A-11}$$

which is the same as Equation (3-28).

APPENDIX II

COMPUTER FLOW DIAGRAM

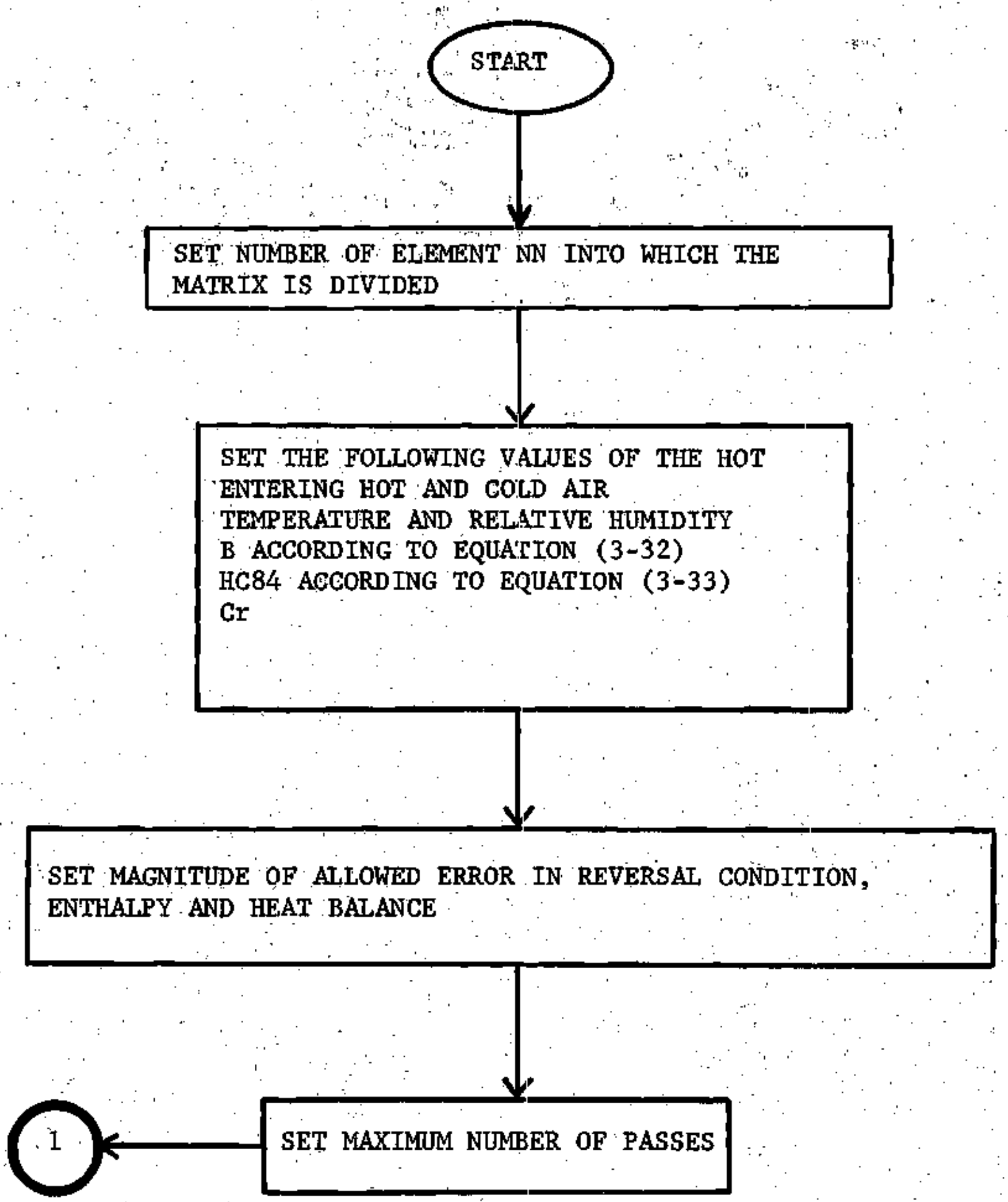

1

CALL SUBROUTINE NUMBER

WRITE TABLES OF RESULTS ACCORDING TO TABLES 2 THROUGH 9

INCREASE THE NUMBER OF ELEMENTS OF THE MATRIX AND REPEAT THE WHOLE THING UP TO HERE

CALCULATE

a) $\frac{C_{min}}{C_{max}}$, $\frac{C_r}{C_{min}}$, NTUo

b) EXTRAPOLATE η TO INFINITE NUMBER OF ELEMENTS

WRITE EVERY VALUE OF THIS BOX

STOP

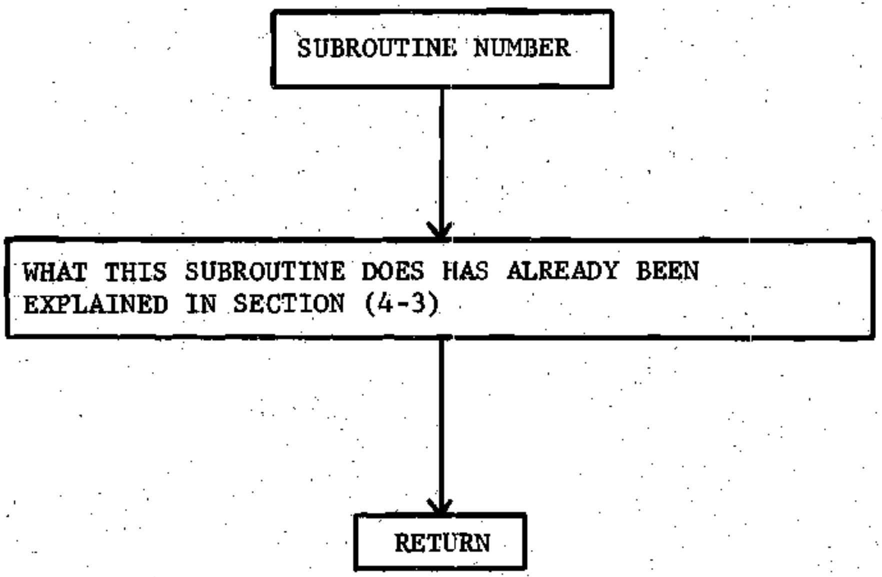
SUBROUTINE NUMBER
WHAT THIS SUBROUTINE DOES HAS ALREADY BEEN EXPLAINED IN SECTION (4-3)
RETURN

BIBLIOGRAPHY

1. Jakob, M., Heat Transfer, Volume II, John Wiley & Sons, Inc., New York, 1957.

2. Hausen, H., "Accomplished Calculations of Heat Exchange in Regenerators," MAP Reports and Translations, no. 312, 1946.

3. Harper, D. B., and Rohsenow, W. M., "Effect of Rotary Regenerator Performance on Gas-Turbine Plant Performance," Trans. ASME, Volume 75, pp. 759-765, 1953.

4. Tong, L. S., and A. L. London, "Heat Transfer and Flow Friction Characteristics of Woven-screen and Crossed-rod Matrices," Trans. ASME, Volume 79, 1957.

5. Coppage, J. E., and A. L. London, "The Periodic Flow Regenerator--A Summary of Design Theory," Trans. ASME, Volume 75, p. 779, 1953.

6. Lamberton, T. J., "Performance Factors of a Periodic-flow Heat Exchanger," Trans. ASME, Volume 80, pp. 586-592, 1958.

7. Kays, W. M., and A. L. London, Compact Heat Exchangers, McGraw-Hill Book Company, New York, 1964.

8. Bahnke, G. D., and C. P. Howard, "The Effect of Longitudinal Heat Conduction on Periodic Flow Heat Exchanger Performance," Trans. ASME, Volume 86, pp. 105-120, 1964.

9. Mercure, R. A., "Design and Test of a Rotary Regenerator for an Electric Clothes Dryer," Report Prepared for Whirlpool Corporation, St. Joseph, Michigan, 1969.

10. Stoecker, W. F., Principles for Air Conditioning Practice, Industrial Press, Inc., New York, 1968.

11. American Society of Mechanical Engineers, Steam Tables, New York, 1967.

12. Zimmerman, O. T., and I. Lavine, Psychrometric Tables and Charts, Industrial Research Service, Inc., Dover, New Hampshire, 1964.